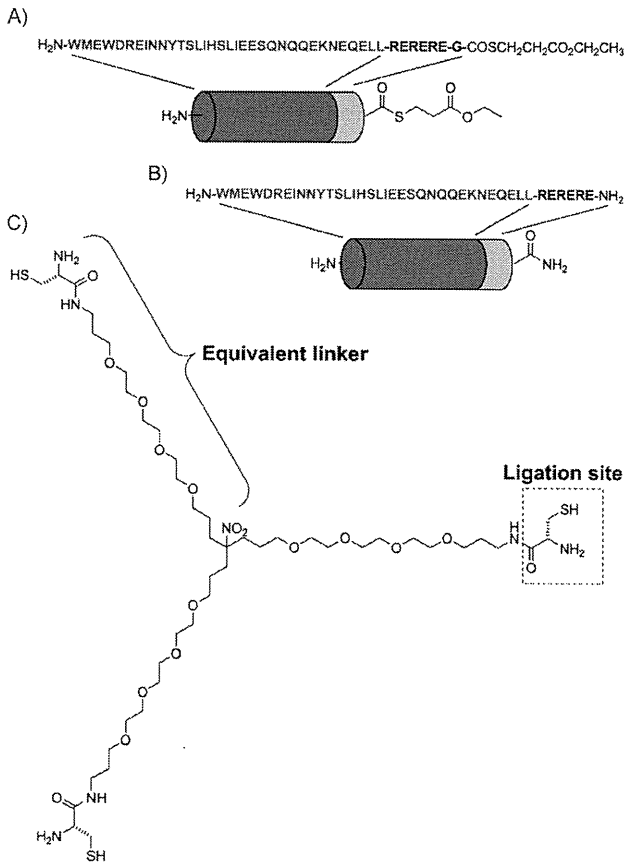


**Figure 1.** C34-derived peptides: A) C34REG-thioester and B) C34REG. C) The design of a C3-symmetric template.

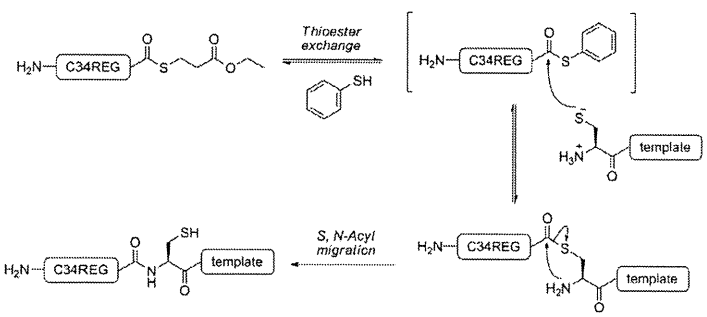


**Figure 2.** The native chemical ligation used for assembly of the C34REG-thioester on the template.

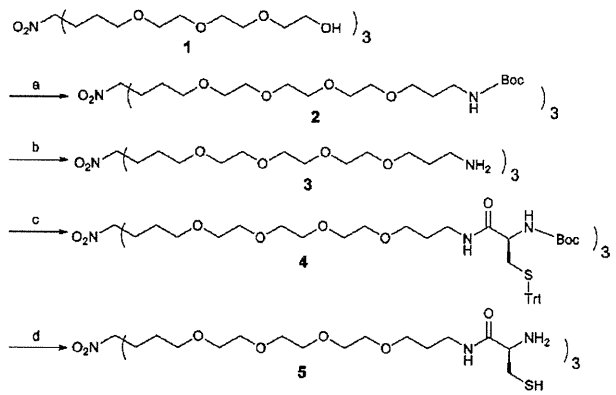

**Scheme 1.** Synthesis of the equivalently branched template **5**. *Reagents and conditions*: a) (3-bromopropyl)carbamic acid *tert*-butyl ester, NaH, THF; b) 4 M HCl/dioxane; c) Boc-Cys(Trt)-OH, EDCI·HCl, HOBt·$H_2O$, $Et_3N$, DMF; d) 90% aq. TFA.

N36 monomer N36RE and the N36 trimer triN36e form a highly structured α helix, and that the helical content of triN36e was greater than that of N36RE.[20,26] These results suggest that in contrast to N36-derived peptides, C34-derived peptides tend to form random structures both in the monomeric and trimeric forms. To assess the interaction of triC34e with N36, CD spectra of a mixture of triC34e with an N36-derived peptide, N36RE, were measured (Figure 3B). The spectrum of the C34REG and N36RE mixture and that of the triC34e and N36RE mixture showed double minima at λ 208 and 222 nm, indicating that the peptide mixture forms an α-helical structure and that the helical content of the trimer triC34e and N36RE mixture is lower than that of the monomer C34REG and N36RE mixture. This is evidence that relative to the monomer C34REG, the trimer triC34e interacts with N36 only with difficulty, due to the assembly of three peptide strands by covalent bonds.

As the trimeric C34 was proven to interact with N36 helices, the potential HIV-1 inhibitory activities of the C-terminal peptides, C34REG and triC34e, were evaluated. The C34 peptide without the solubility-increasing sequence (3×[Arg-Glu], obtained from NIAID) was used as the monomeric control.[27] All peptides showed potent inhibitory activity in the viral fusion assay (Table 1), with the potency of triC34e being 100- and 40-fold higher than that of C34REG and C34 peptides, respectively. Notably, the triC34e trimer peptide is remarkably more potent in anti-HIV-1 activity than the monomer, indicating that a trimeric form is critical for inhibitory activity. Cytotoxicity from the peptides was not observed at concentrations of 15 μM for C34REG and C34, and 5 μM for triC34e.

We next carried out an assay for the inhibition of viral replication. As shown in Table 2, triC34e showed 30- and 20-fold higher inhibitory activity than peptides C34 and C34REG, respectively. In the two anti-HIV-1 assays, triC34e showed a great enhancement of activity over the C34 monomers. The $IC_{50}$ values obtained in the assays are different, and this can be

**Table 1.** $IC_{50}$ and $CC_{50}$ values determined by viral fusion inhibition and cell viability assays.

| | C34 peptide[a] | C34REG | triC34e |
|---|---|---|---|
| $IC_{50}$ [μM][b] | 0.044 | 0.12 | 0.0013 |
| $CC_{50}$ [μM][c] | >15 | >15 | >5 |

[a] HIV-1 IIIB C34 peptide. [b] $IC_{50}$ values are based on luciferase signals in TZM-bl cells infected with HIV-1 (NL4-3 strain). [c] $CC_{50}$ values are based on the decrease in viability of TZM-bl cells. All data are the mean values from at least three experiments.

  

| Table 2. $IC_{50}$ values determined by inhibition assay based on p24 ELISA. | | | |
|---|---|---|---|
| | C34 peptide | C34REG | triC34e |
| $IC_{50}$ [μM][a] | 1.59 | 1.06 | 0.0547 |

[a] $IC_{50}$ values are based on the production of p24 in MT-4 cells infected with HIV-1 (NL4-3 strain). All data are the mean values from at least three experiments.

explained through differences in experimental procedures. In the fusion inhibition assay, cells were treated with peptides before viral infection. In contrast, in the viral replication inhibition assay, peptides were treated after viral adsorption to cells. Therefore, in the latter case, the infection by HIV-1 might precede peptide binding to gp41.

It has been shown that T-1249, an analogue of enfuvirtide, and its hydrophobic C-terminal region inhibit HIV-1 fusion by interacting with lipid bilayers.[28] The tryptophan-rich domain of T-1249 was shown to play important roles in HIV-1 fusion.[29–31] As enfuvirtide shows weak interaction with the gp41 core structure, and the C34 sequence lacks the C-terminal lipid binding domain, it has been suggested that C34 has a mechanism of action distinct from that of enfuvirtide.[32] Thus, it is of interest to discern the mechanism of the enhanced inhibition observed with triC34e relative to the monomer. Two explanations can be envisaged: 1) the α helicity of the C34 trimer is higher than that of the monomer, as shown in Figure 3A, and as a result, the C34 trimer binds more strongly to the N36 trimer; and 2) in the mixture with the N36 monomer, the C34 trimer shows less α helicity than its monomer (Figure 3B). As shown in Figure 3A, the molar ellipticity at 222 nm is similar for both the C34 trimer and the monomer. Thus, the decrease at 222 nm in the mixture with N36 might be due to a decrease in the α helicity of N36. These results suggest that the C34 trimer might destabilize helix formation in N36 and thus exert potent inhibitory activity. It has been shown that a dimeric C37 (residues 625–661) variant does not show a significant difference in $IC_{50}$ value against HIV-1 from wild-type C37, although the dimeric peptide shows tighter binding to the gp41 N-HR coiled-coil than the C37 monomer.[33] Thus, the mechanism of action of the C34 trimer could be different from that of the dimeric C-peptide. The detailed action mechanism of the trimer as a fusion inhibitor and the reasons behind its remarkable increased anti-HIV-1 activity will be the subjects of future studies in our research group.

A C-terminal helical peptide of HIV-1 gp41 has been designed as a new HIV fusion inhibitor and was synthesized with a novel template and three branched linkers of equal length. The native chemical ligation proceeded by chemoselective coupling in an aqueous medium of an unprotected C34 derivative containing a C-terminal thioester with a three-cysteine-armed scaffold. This process led to the production of triC34e. As a fusion inhibitor, triC34e has potent anti-HIV-1 activity, 100-fold greater than that of the C34REG monomer, although the anti-HIV-1 activity of the N36 trimer is threefold higher than that of the N36 monomer, and the N36 content is the same in both cases.[20] A trimeric form of C34 is evidently critical as the

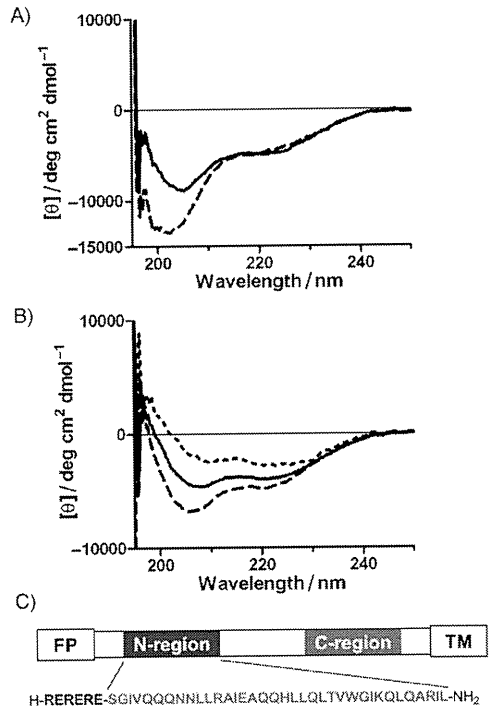


**Figure 3.** A) CD spectra of C34REG (monomer, -----, 6 μM) and triC34e (trimer, ——, 2 μM). B) CD spectra in the presence or absence of the N36 monomer N36RE:[20] -----, [C34REG (6 μM) + N36RE (6 μM)]; ——, [triC34e (2 μM) + N36RE (6 μM)]; •••••, N36RE (6 μM). In the amino acid sequence of N36RE, the triplet repeat of arginine and glutamic acid is located at the N-terminus of the original N36 sequence.[20] C) Amino acid sequence of N36RE: FP and TM represent the hydrophobic fusion peptide and transmembrane domains, respectively.

active structure of the fusion inhibitor. The soluble C34 derivative, SC34, retains potent inhibitory effects against enfuvirtide-resistant viruses,[34] and this suggests that the present highly potent trimeric inhibitor could be effective for enfuvirtide-resistant HIV-1 strains. The design of inhibitors that target the dynamic supramolecular mechanism of HIV-1 fusion will be useful for future studies of anti-HIV-1 agents.

## Experimental Section

### *Conjugation of C34REG-thioester and the template to produce triC34e*

TCEP·HCl (773 μg, 2.67 μmol) and thiophenol (9 μL, 89 μmol) were dissolved in 0.1 M sodium phosphate buffer (60 μL) containing 6 M urea and EDTA (pH 8.5, 2 mM) under a nitrogen atmosphere. Compound **5** (100 μg, 0.0899 μmol), C34REG-thioester (1.77 mg, 0.297 μmol), and $CH_3CN$ (20 μL) were added. The reaction was stirred for 5 h at 37 °C and monitored by HPLC. The ligation product (triC34e) was separated as an HPLC peak and characterized by ESI-ToF-MS (*m/z* calcd for $C_{703}H_{1108}N_{205}O_{245}S_6$ $[M+H]^+$: 16533.9, found: 16543.8). Purification was performed by reversed-phase HPLC (Cosmosil 5 $C_{18}$-AR II column, 10×250 mm, Nacalai Tesque, Inc.) with elution using a 33–43% linear gradient of $CH_3CN$ (0.1% TFA) over 40 min. Purified triC34e, obtained in 17% yield, was identified by ESI-ToF-MS. Details of the synthesis of these peptides are described in the Supporting Information.

  

### CD spectra

Circular dichroism measurements were performed with a J-720 CD spectropolarimeter equipped with a thermoregulator (Jasco). The wavelength dependence of molar ellipticity [$\theta$] was monitored at 25 °C from $\lambda$ 195 to 250 nm. The peptides were dissolved in PBS (50 mM sodium phosphate, 150 mM NaCl, pH 7.2).

### Virus preparation

For virus preparation, 293FT cells in a 60 mm dish were transfected with the pNL4-3 construct (10 μg) by the calcium phosphate method. The supernatant was collected 48 h after transfection, passed through a 0.45 μm filter, and stored at −80 °C as the virus stock.

### Anti-HIV-1 assay

For the viral fusion inhibition assay, TZM-bl cells ($2\times10^4$ cells per 100 μL) were cultured with the NL4-3 virus (5 ng of p24) and serially diluted peptides. After culture for 48 h, cells were lysed, and the luciferase activity was determined with the Steady-Glo luciferase assay system (Promega, Fitchburg, WI, USA).[35] For the viral replication inhibition assay, MT-4 cells ($5\times10^4$ cells) were exposed to HIV-1 NL4-3 (1 ng of p24) at 4 °C for 30 min. After centrifugation, cells were resuspended with 150 μL medium containing indicated concentrations of serially diluted peptides. Cells were cultured at 37 °C for 3 days, and the concentration of p24 in the culture supernatant was determined by HIV-1 p24 antigen ELISA kit (ZeptoMetrix, Buffalo, NY, USA).

### Cytotoxicity assay

The cytotoxic effects of peptides were determined by the CellTiter 96 AQueous One Solution Cell Proliferation assay system (Promega) under the same conditions, but in the absence of viral infection.

## Acknowledgements

*The following reagent was obtained through the US National Institutes of Health (NIH) AIDS Research and Reference Reagent Program, Division of AIDS, NIAID, NIH: HIV-1 IIIB C34 Peptide from DAIDS, NIAID. This work was supported in part by a Grant-in-Aid for Scientific Research from the Ministry of Education, Culture, Sports, Science, and Technology of Japan, and Health and Labour Sciences Research Grants from the Japanese Ministry of Health, Labor, and Welfare. C.H. is supported by JSPS research fellowships for young scientists.*

**Keywords:** antiviral agents · C34 trimers · fusion inhibitors · gp41 · HIV-1

[1] C. Hashimoto, T. Tanaka, T. Narumi, W. Nomura, H. Tamamura, *Expert Opin. Drug Discovery* **2011**, *6*, 1067–1090.
[2] E. O. Freed, M. A. Martin, *J. Biol. Chem.* **1995**, *270*, 23883–23886.
[3] D. M. Eckert, P. S. Kim, *Annu. Rev. Biochem.* **2001**, *70*, 777–810.
[4] R. Wyatt, J. Sodroski, *Science* **1998**, *280*, 1884–1888.
[5] E. A. Berger, P. M. Murphy, J. M. Farber, *Annu. Rev. Immunol.* **1999**, *17*, 657–700.
[6] M. Lu, S. C. Blacklow, P. S. Kim, *Nat. Struct. Biol.* **1995**, *2*, 1075–1082.
[7] S. Jiang, K. Lin, N. Strick, A. R. Neurath, *Nature* **1993**, *365*, 113.
[8] C. T. Wild, D. C. Shugars, T. K. Greenwell, C. B. McDanal, T. J. Matthews, *Proc. Natl. Acad. Sci. USA* **1994**, *91*, 9770–9774.
[9] C. T. Wild, T. Oas, C. McDanal, D. Bolognesi, T. Matthews, *Proc. Natl. Acad. Sci. USA* **1992**, *89*, 10537–10541.
[10] J. M. Kilby, S. Hopkins, T. M. Venetta, B. DiMassimo, G. A. Cloud, J. Y. Lee, L. Alldredge, E. Hunter, D. Lambert, D. Bolognesi, T. Matthews, M. R. Johnson, M. A. Nowak, G. M. Shaw, M. S. Saag, *Nat. Med.* **1998**, *4*, 1302–1307.
[11] J. M. Kilby, J. J. Eron, *N. Engl. J. Med.* **2003**, *348*, 2228–2238.
[12] J. P. Lalezari, K. Henry, M. O'Hearn, J. S. Montaner, P. J. Piliero, B. Trottier, S. Walmsley, C. Cohen, D. R. Kuritzkes, J. J. Eron, Jr., J. Chung, R. DeMasi, L. Donatacci, C. Drobnes, J. Delehanty, M. Salgo, *N. Engl. J. Med.* **2003**, *348*, 2175–2185.
[13] S. Liu, W. Jing, B. Cheng, H. Lu, J. Sun, X. Yan, J. Niu, J. Farmar, S. Wu, S. Jiang, *J. Biol. Chem.* **2007**, *282*, 9612–9620.
[14] D. C. Chan, D. Fass, J. M. Berger, P. S. Kim, *Cell* **1997**, *89*, 263–273.
[15] E. De Rosny, R. Vassell, R. T. Wingfield, C. T. Wild, C. D. Weiss, *J. Virol.* **2001**, *75*, 8859–8863.
[16] J. P. Tam, Q. Yu, *Org. Lett.* **2002**, *4*, 4167–4170.
[17] W. Xu, J. W. Taylor, *Chem. Biol. Drug Des.* **2007**, *70*, 319–328.
[18] J. M. Louis, I. Nesheiwat, L. Chang, G. M. Clore, C. A. Bewlet, *J. Biol. Chem.* **2003**, *278*, 20278–20285.
[19] E. Bianch, J. G. Joyce, M. D. Miller, A. C. Finnefrock, X. Liang, M. Finotto, P. Ingllinella, P. McKenna, M. Citron, E. Ottinger, R. W. Hepler, R. Hrin, D. Nahas, C. Wu, D. Montefiori, J. W. Shiver, A. Pessi, P. S. Kim, *Proc. Natl. Acad. Sci. USA* **2010**, *107*, 10655–10660.
[20] T. Nakahara, W. Nomura, K. Ohba, A. Ohya, T. Tanaka, C. Hashimoto, T. Narumi, T. Murakami, N. Yamamoto, H. Tamamura, *Bioconjugate Chem.* **2010**, *21*, 709–714.
[21] M. Lu, H. Ji, S. Shen, *J. Virol.* **1999**, *73*, 4433–4438.
[22] D. M. Eckert, P. S. Kim, *Proc. Natl. Acad. Sci. USA* **2001**, *98*, 11187–11192.
[23] E. Bianchi, M. Finotto, P. Ingallinella, R. Hrin, A. V. Carella, X. S. Hous, W. A. Schleif, M. D. Miller, *Proc. Natl. Acad. Sci. USA* **2005**, *102*, 12903–12908.
[24] P. E. Dawson, T. W. Muir, I. Clark-Lewis, S. B. H. Kent, *Science* **1994**, *266*, 776–779.
[25] P. E. Dawson, M. J. Churchill, M. R. Ghadiri, S. B. H. Kent, *J. Am. Chem. Soc.* **1997**, *119*, 4325–4329.
[26] D. C. Chan, C. T. Chutkowski, P. S. Kim, *Proc. Natl. Acad. Sci. USA* **1998**, *95*, 15613–15617.
[27] S. A. Gallo, K. Sackett, S. S. Rawat, Y. Shai, R. Blumenthal, *J. Mol. Biol.* **2004**, *340*, 9–14.
[28] A. S. Veiga, N. C. Santos, L. M. Loura, A. Fedorov, M. A. Castanho, *J. Am. Chem. Soc.* **2004**, *126*, 14758–14763.
[29] M. K. Lawless, S. Barney, K. I. Guthrie, T. B. Bucy, S. R. Petteway, Jr., G. Merutka, *Biochemistry* **1996**, *35*, 13697–13708.
[30] K. Salzwedel, J. T. West, E. Hunter, *J. Virol.* **1999**, *73*, 2469–2480.
[31] S. G. Peisajovich, S. A. Gallo, R. Blumenthal, Y. Shai, *J. Biol. Chem.* **2003**, *278*, 21012–21017.
[32] S. Liu, H. Lu, Y. Xu, S. Wu, S. Jiang, *J. Biol. Chem.* **2005**, *280*, 11259–11273.
[33] K. M. Kahle, K. Steger, M. J. Root, *PLoS Pathog.* **2009**, *5*, e1000674.
[34] A. Otaka, M. Nakamura, D. Nameki, E. Kodama, S. Uchiyama, S. Nakamura, H. Nakano, H. Tamamura, Y. Kobayashi, M. Matsuoka, N. Fujii, *Angew. Chem.* **2002**, *114*, 3061–3064; *Angew. Chem. Int. Ed.* **2002**, *41*, 2937–2940.
[35] E. J. Platt, K. Wehrly, S. E. Kuhmann, B. Chesebro, D. Kabat, *J. Virol.* **1998**, *72*, 2855–2864.

Received: November 22, 2011
Revised: December 15, 2011
Published online on January 13, 2012

  

AIDS RESEARCH AND HUMAN RETROVIRUSES
Volume 27, Number 00, 2011

DOI: 10.1089/aid.2011.0180

# The Hematopoietic Cell-Specific Rho GTPase Inhibitor ARHGDIB/D4GDI Limits HIV Type 1 Replication

Tadashi Watanabe,[1] Emiko Urano,[2] Kosuke Miyauchi,[2] Reiko Ichikawa,[2] Makiko Hamatake,[2] Naoko Misawa,[1] Kei Sato,[1] Hirotaka Ebina,[1] Yoshio Koyanagi,[1] Jun Komano[2]

## Abstract

Rho GTPases are able to influence the replication of human immunodeficiency virus type 1 (HIV-1). However, little is known about the regulation of HIV-1 replication by guanine nucleotide dissociation inhibitors (GDIs), one of the three major regulators of the Rho GTPase activation cycle. From a T cell-based cDNA library screening, ARHGDIB/RhoGDI$\beta$, a hematopoietic lineage-specific GDI family protein, was identified as a negative regulator of HIV-1 replication. Up-regulation of ARHGDIB attenuated the replication of HIV-1 in multiple T cell lines. The results showed that (1) a significant portion of RhoA and Rac1, but not Cdc42, exists in the GTP-bound active form under steady-state conditions, (2) ectopic ARHGDIB expression reduced the F-actin content and the active forms of both RhoA and Rac1, and (3) HIV-1 infection was attenuated by either ectopic expression of ARHGDIB or inhibition of the RhoA signal cascade at the HIV-1 Env-dependent early phase of the viral life cycle. This is in good agreement with the previous finding that RhoA and Rac1 promote HIV-1 entry by increasing the efficiency of receptor clustering and virus-cell membrane fusion. In conclusion, the ARHGDIB is a lymphoid-specific intrinsic negative regulator of HIV-1 replication that acts by simultaneously inhibiting RhoA and Rac1 functions.

## Introduction

The human immunodeficiency virus type 1 (HIV-1) is the causative agent of acquired immunodeficiency syndrome (AIDS). The clinical success of Maraviroc, an antiretroviral drug that targets the host cell protein CCR5, demonstrates the importance of understanding host-HIV-1 interaction as this information will provide the basis for the development of the next generation of antiretroviral drugs. HIV-1 replicates primarily in CD4-positive T cells. However, aside from the viral receptors CD4 and CCR5, few lymphoid cell-specific regulators of HIV-1 replication have been identified. This is partly due to the use of nonlymphoid cells to screen for cellular factors that regulate HIV-1 replication, as these cells support the efficient transduction of genetic materials. Therefore, T cell-based cDNA library screening has some advantages, as discussed later.

Members of the Rho GTPase family, including RhoA, Rac1, and Cdc42, have been reported to regulate the replication of HIV-1 at various stages of the viral life cycle, including viral entry, transcription, and viral release.[1–7] Although these proteins are widely expressed, genome-wide screens for proteins that regulate HIV-1 replication using siRNA or shRNA libraries have failed to identify Rho GTPases.[8–10] This may suggest that Rho GTPases are not potent regulators of HIV-1 replication and are therefore difficult to detect unless the viral replication assay is employed, since multiple replication cycles augment the biological effects of Rho GTPases.

There are three major regulators of the activation cycle of Rho GTPases: guanine nucleotide exchange factors (GEFs), GTPase-activating proteins (GAPs), and guanine nucleotide dissociation inhibitors (GDIs or ARHGDIs). RhoGEFs promote the exchange of GDP for GTP, RhoGAPs accelerate GTP hydrolysis, and ARHGDIs stabilize the GDI-bound form of Rho GTPases and also mask the lipid moiety of Rho GTPases, thereby sequestering Rho GTPases at the plasma membrane.[11–14] Some RhoGAPs and RhoGEFs have been known to regulate HIV-1 replication.[6,9,10,15–18] Positive regulators of Rho GTPases, such as RhoGEFs, were identified in the genome-wide screens, although these studies yielded varying results. In this sense, the upstream regulators of Rho GTPases may more potently influence HIV-1 replication than Rho GTPases themselves when expression levels are dysregulated. ARHGDIs have yet to be identified as regulators of HIV-1 replication.

[1]Laboratory of Viral Pathogenesis, Institute for Virus Research, Kyoto University, Kyoto, Japan.
[2]AIDS Research Center, National Institute of Infectious Diseases, Tokyo, Japan.

Previously, we established a genetic screening system using a T cell-derived cDNA library to isolate cellular factors that render cells resistant to HIV-1 replication.[19,20] This system is unique in that the screen is based on MT-4 cells, a human CD4-positive T cell line, which were exposed to replication-competent HIV-1. Using this system, the carboxy-terminal domains of Brd4 and SEC14L1a were found to be negative regulators of HIV-1 replication.[19,20] Importantly, these factors were not found in previous genetic screens, suggesting that our system complements other genome-wide analyses. In this study, we describe a lymphoid-specific RhoGDI that negatively regulates HIV-1 replication through attenuation of both RhoA and Rac1 functions.

## Materials and Methods

### *Cells*

Cells were maintained in RPMI 1640 medium (Sigma, St. Louis, MO) supplemented with 10% fetal bovine serum (FBS; Japan Bioserum, Tokyo, Japan or Thermo Fisher Scientific Inc., Waltham, MA), 50–100 U/ml penicillin, and 50–100 $\mu$g/ml streptomycin (Invitrogen, Tokyo, Japan), and then incubated at 37°C in a humidified 5% $CO_2$ atmosphere. The selection of cDNA library-transduced cells was described previously.[20] To select puromycin-resistant cells after infection with pQc- or pSM2c-based murine leukemia virus (MLV) vector, 1 $\mu$g/ml puromycin (Sigma) was added to the culture medium.

### *Plasmids*

The plasmid vectors pCMMP, pMDgag-pol, pSV-tat, phRL/CMV, and pVSV-G were described previously.[21] The shRNA expression vectors pSM2c and pSM2/ARHGDIB (RHS1764-9680880) were purchased from Thermo Fisher Scientific (Open Biosystems Products, Huntsville, AL). The pQcXIP was obtained from Clontech (BD Biosciences Clontech, Palo Alto, CA). pGEX-Rhotekin-RBD and pGEX-4T-PAK2-RBD were kindly provided by S. Narumiya, Kyoto University.[3,22] To construct pLTR-hRL, the HIV-$1_{HXB2}$ long terminal repeat (LTR) was amplified by PCR using the following primers: 5′-GGA TCC TGG AAG GGC TAA TTC ACT CC-3′ and 5′-GCT AGC TGC AGC TGC TAG AGA TTT TCC ACA CTG-3′. The *BglII-NheI* fragment of the PCR product was cloned into the corresponding restriction sites of phRL/CMV, generating pLTR-hRL. The LTR-Luc plasmid was described previously.[23] To construct pCMV-Tat-FLAG, HIV-$1_{NL4-3}$ *tat* was amplified from cDNA prepared from HIV-1-infected MT-4 cells by RT-PCR using the following primers: 5′-ATG GAG CCA GTA GAT CCT AGA CTA GAG CCC T-3′ and 5′-TTC CTT CGG GCC TGT CGG GT-3′. The PCR product was cloned into the *Eco*RV sites of pcDNA3.1 Zeo(+) bearing FLAG-tags at the *NotI-XhoI* site (Invitrogen). The pCMV-Luc plasmid was a generous gift from Dr. Hijikata (Kyoto University).

### *Flow cytometry*

Cells were incubated with anti-CD4, anti-CD8, or anti-CXCR4 monoclonal antibodies conjugated to R-phycoerythrin (PE; BD Pharmingen, San Diego, CA) for 30 min at 4°C. Cells were washed once with phosphate-buffered saline (PBS) supplemented with 1% FBS and analyzed by FACS Calibur (Beckton Dickinson, San Jose, CA).

### *Phalloidin staining of F-actin*

Phalloidin staining of F-actin was performed as described previously.[24] In brief, cells were fixed, permeabilized by cytofix/cytoperm (BD Bioscience) for 20 min on ice, washed, and stained with Alexa Fluor 647-phalloidin (Invitrogen) for 30 min at 4°C. Samples were kept on ice until analysis by FACS Calibur or Canto II (Beckton Dickinson, San Jose, CA). The flow cytometric data were analyzed using FlowJo version 9.3 (Tree-star Inc., Ashland, OR).

### *Viruses*

The retroviral vector pCMMP, carrying the MT-4 cDNA library and a green fluorescent protein (GFP) expression cassette, was obtained from Takara (Takara, Otsu, Japan). Full-length ARHGDIB was cloned from a lymph node cDNA library (Takara) by RT-PCR using the primers 5′-GCA CCG GTC TCG AGC CAC CAT GAC TGA AAA AGC CCC AGA GC-3′ and 5′-CCA ATT GGA TCC TCA TTC TGT CCA CTC CTT CTT AAT CG-3′, and cloned into the pCMMP vector. The MLV vectors were produced by tripartite transfection of pMDgag-pol, pVSV-G, and either pCMMP, pQc, or pSM2c retroviral vector. Cells were infected with the MLV vectors as described previously.[21] The production of replication-competent HIV-$1_{HXB2}$ and the measurement of replication kinetics were performed as described previously.[21]

### *Western blotting*

Western blotting was performed according to techniques described previously.[25] The following monoclonal antibodies were used: anti-RhoA (C-11; Santa Cruz Biotechnology, Santa Cruz, CA), anti-Rac1 (23A8; Millipore, Japan), anti-Cdc42 (B-8; Santa Cruz Biotechnology), anti-ARHGDIB (A01; Abnoba, Taiwan), anti-$p24^{CA}$ (183-H12-5C; NIH AIDS Research and Reference Reagent Program), anti-actin (clone C4; Millipore), and anti-tubulin (DM1A; Sigma). Densitometric analysis was performed using ImageJ ver. 1.43 software (obtained from http://rsbweb.nih.gov/ij/index.html).

### *Active Rho GTPase capture assay*

We adopted a protocol described previously.[3,22] In brief, the glutathione *S*-transferase (GST) fused to the Rho GTPase binding domain (RBD) of Rhotekin and GST fused to the RBD of PAK2 were expressed in *E. coli* and purified by incubating the cell lysates with glutathione-Sepharose 4B beads (GE Healthcare Bio-Sciences, Piscataway, NJ) for 3 h at 4°C. The beads were washed three times with ice-cold Rho buffer (25 mM HEPES, pH 7.5, 150 mM NaCl, 10 mM $MgCl_2$, 1 mM EDTA, 10% Glycerol). Finally, the beads were washed with ice-cold Rho buffer supplemented with 1% NP-40 and protease inhibitor cocktail tablets (Complete, Roche Diagnostics GmbH, Mannheim, Germany). Cells were incubated in ice-cold Rho buffer for 15 min on ice, and the cell lysates were clarified by centrifugation at 18,000 × *g* at 4°C for 20 min. A fraction of the cleared cell lysates was incubated at 37°C for 30 min as a negative control or coincubated with GTP$\gamma$S (0.1 mM, Sigma) for 30 min at 30°C as a positive control. These preparations were incubated with the above beads at 4°C for 1 h. The beads were washed three times with Rho buffer containing 1% NP-40 and subjected to SDS-PAGE followed by Western blotting. The bead-bound GTPases were detected

using a monoclonal antibody against RhoA, Rac1, or Cdc42, as appropriate.

*Single-round infection assay*

Single-round virus infection and luciferase assays were performed as described previously.[21,26] In brief, cells were exposed to viral preparations containing 1–10 ng of $p24^{CA}$. Luciferase activities were measured at 2–3 days postinfection with the Picagene luciferase assay kit (Toyo Ink, Tokyo, Japan) or Steady-Glo kit (Promega, Tokyo, Japan) according to the manufacturer's protocols. For the inhibition of Rho-kinase (ROCK), cells were pretreated with 12.5 $\mu$M Y27632 (Nakalai tesque, Kyoto, Japan) for 1 h and incubated with the viral preparation in the presence of 12.5 $\mu$M Y27632 for 4 h. Cells were washed with tissue culture medium and cultivated for 2 days. Light emission was detected with a 1420 ARVOSX multilabel counter (Perkin Elmer, Wellesley, MA) or a Veritas luminometer (Promega).

*Single-round production assay*

Five million PM1/control or PM1/ARHGDIB cells were resuspended in 250 $\mu$l of STBS (25 mM Tris-Cl, pH 7.4, 137 mM NaCl, 5 mM KCl, 0.6 mM $Na_2HPO_4$, 0.7 mM $CaCl_2$, and 0.5 mM $MgCl_2$), including 10 $\mu$g of pHXB2 proviral plasmid DNA. Cells were mixed with 250 $\mu$l of STBS containing 1 mg/ml of DEAE-Dextran and incubated for 30 min at room temperature (RT). The cells were then incubated with STBS containing 10% DMSO for 2 min at RT and washed with 1 ml HBSS (Invitrogen). Transfected cells were cultured in RPMI medium containing 10% FBS and 1 $\mu$M efavirenz. After 2 days in culture, viruses in the culture supernatant were pelleted by ultracentrifugation on a 20% sucrose cushion. Cells and viruses were lysed with radioimmunoprecipitation assay (RIPA) lysis buffer (0.05 M Tris-HCl, 0.15 M NaCl, 1% Triton X-100, 0.1% sodium dodecyl sulfate, and 1% sodium deoxycholate) and electrophoresed in a 10% polyacrylamide gel for SDS–PAGE. Proteins were then transferred to a PVDF membrane, and $p24^{CA}$ was detected by immunoblot analysis using an anti-$p24^{CA}$ antibody.

*Reporter expression assay*

The luciferase-expressing reporter plasmids were transfected into PM1 cells according to the DEAE-Dextran method as described above. For transfection, either 1 $\mu$g of pCMV-Luc, 10 $\mu$g of pLTR-Luc, 0.5 $\mu$g of phRL/CMV, or 1 $\mu$g of pLTR-hRL was used. The pLTR-Luc and pLTR-hRL were co-transfected with 5 $\mu$g of pCMV-tat-FLAG and 1 $\mu$g of pSVtat, respectively. Firefly luciferase activity was measured as described above. Renilla luciferase activity was also measured as described above, except that the Renilla Luciferase Assay System (Promega) was used in place of the Steady-Glo kit. The data were analyzed using a two-tailed Student's *t*-test.

## Results

*Identification of RhoGDIβ/ARHGDIB as a negative regulator of HIV-1 replication*

A pool of MT-4 cells constitutively expressing a cDNA library transduced with an MLV-based retroviral vector was used to screen for possible regulators of HIV-1 replication. The MLV vector carried an expression cassette for GFP and inserts from a cDNA library derived from MT-4 cells (Fig. 1A). The cDNA-transduced cells were enriched with a cell sorter using GFP as a marker. These cells were then infected with CXCR4-using (X4) $HIV\text{-}1_{HXB2}$. MT-4 cells have been shown to support efficient HIV-1 production and rapidly undergo cell death after infection. The surviving MT-4 cells were propagated and genomic DNA was isolated to identify the inserted cDNA, as described previously.[19] These genes were considered potential negative regulators of HIV-1 replication. A cDNA clone encoding ARHGDIB (RhoGDI$\beta$/LyGDI/D4GDI; gene ID 397) was recovered from the MT-4 cDNA library (1/94 independent clones, 1.1%).

Full-length ARHGDIB cDNA was cloned into the MLV vector pQcXIP, and a T cell line expressing ARHGDIB at levels higher than endogenous levels was established. To verify the HIV-1-resistant phenotype of ARHGDIB, the rate of HIV-1 replication was assessed in MT-4 cells subjected to ectopic ARHGDIB expression. In these cells, ARHGDIB levels were increased by approximately 4.9-fold compared with control cells, while the cell surface expression of CD4 and CXCR4 was not significantly affected in MT-4 cells (Fig. 1B). Even the modest up-regulation of ARHGDIB delayed HIV-1 replication kinetics (Fig. 1B). Suppression of HIV-1 replication was independently reproduced in MT-4 cells, even when a different retroviral vector, pCMMP, was used to transduce ARHGDIB (data not shown). In addition, neither the rate of cell proliferation nor cell morphology was affected by stable ectopic expression of ARHGDIB over at least 6 months in culture (data not shown). Delayed HIV-1 replication in cells ectopically overexpressing ARHGDIB was also observed in PM1 (Fig. 1C), M8166 (Fig. 1D), and Jurkat cells (Fig. 1E), in which ARHGDIB levels were increased by 2.1-, 1.9-, and 1.5-fold, respectively, compared with control levels. Similar data were also obtained in SUP-T1 cells (data not shown). The delayed HIV-1 replication in cells ectopically expressing ARHGDIB was reproduced in 10 independent experiments ($p < 0.01$, two-sided binomial test), strongly suggesting that ARHGDIB attenuates the replication of HIV-1. These results indicate that enhanced expression of ARHGDIB renders cells resistant to HIV-1 replication. Consistent with these data, the shRNA-mediated down-regulation of ARHGDIB accelerated the replication of HIV-1 in MT-4 cells (Fig. 1F). These data support the idea that ARHGDIB is a negative regulator of HIV-1 replication.

The RhoGDI family has three members, $\alpha$, $\beta$, and $\gamma$, which correspond to ARHGDI A, B, and C, respectively.[11] RhoGDI family members are known to regulate Rho GTPases, including RhoA, Rac1, and Cdc42, although some nonredundant functions of RhoGDIs have been reported.[27] ARHGDIB/RhoGDI$\beta$ is primarily expressed in cells of a hematopoietic lineage. Given that Rho GTPases are known to be positive regulators of HIV-1 replication and that ARHGDIB is a negative regulator of Rho GTPases in hematopoietic cells, the function of ARHGDIB was investigated in further detail.

*Molecular mediators in the inhibition of HIV-1 replication by ARHGDIB*

Under *in vitro* culture conditions, T cell lines show a constitutively activated cell phenotype, and Rho GTPases, including RhoA, Rac1, and Cdc42, have been implicated in T cell

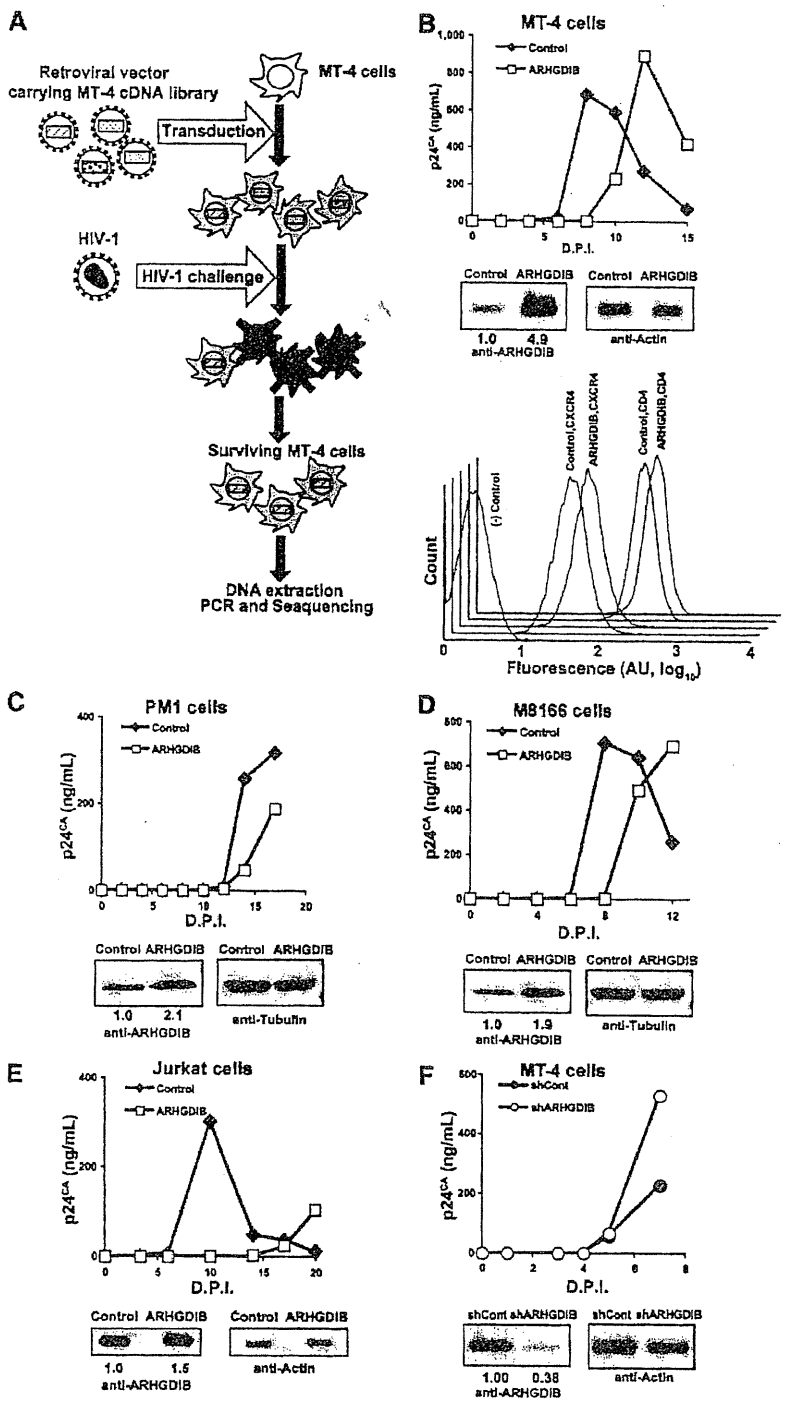


FIG. 1. Isolation and characterization of ARHGDIB as a negative regulator of HIV-1 replication. (A) The screening strategy used to isolate genes that render MT-4 cells resistant to HIV-1 replication. (B–E) Ectopic expression of ARHGDIB (open rectangles) in MT-4 (B), PM1 (C), M8166 (D), and Jurkat (E) cells delayed the replication kinetics of HIV-1. Representative data from five, two, and two independent experiments for MT-4, M8166, and Jurkat cells are shown, respectively. The control counterpart is shown as filled diamonds. (B) The flow cytometric profiles of MT-4 cell surface CD4 and CXCR4 are shown. MT-4/ARHGDIB cells stained for CD8 were used as a negative control. (F) Down-regulation of ARHGDIB (open circles) in MT-4 cells accelerated the replication of HIV-1. The control counterpart is shown as filled circles. (B–F) Expression levels of ARHGDIB and an internal control, either actin or tubulin, were assessed by Western blot analysis. The magnitude of ARHGDIB up- or down-regulation was determined by densitometry and is indicated below each image. AU, arbitrary unit; D.P.I., days postinfection.

activation.[28–30] These Rho GTPases are expressed in various T cell lines, including MT-4, PM1, and M8166 cells, as confirmed by RT-PCR analysis (data not shown). It seemed likely that augmented ARHGDIB expression affected HIV-1 replication by modulating the activity of these Rho GTPases. Thus, the activation status of RhoA, Rac1, and Cdc42 was determined in relation to the enhanced expression of ARHGDIB.

Rho GTPases are intrinsically inefficient hydrolyzing enzymes that quickly cycle between GTP-bound active and GDP-bound inactive forms. If ARHGDIB attenuates HIV-1 replication by inhibiting Rho GTPase activities, some fraction of Rho GTPases would exist in a GTP-bound active form under steady-state tissue culture conditions, and this population should be decreased in cells ectopically expressing ARHGDIB. Using an active Rho GTPase capture assay, the levels of active Rho GTPases in control and ARHGDIB-expressing cells were measured (Fig. 2A). In this assay, GTP-bound Rho GTPase is captured by glutathione-Sepharose beads conjugated to GST fused to the Rho binding domain of Rhotekin or PAK2. The active forms of both RhoA and Rac1, but very little Cdc42, were detected in PM1 cells under steady-state tissue culture conditions (Fig. 2B–D). Activation levels under the steady-state conditions were estimated by comparing the captured Rho GTPase signals with the maximal activation levels, which were established by converting all Rho GTPases to an active form by GTPγS before the pull-down procedure. The activated fractions of Rac1, RhoA, and Cdc42 were 34.2%, 23.2%, and 0.0%, respectively (Fig. 2B–D). Importantly, ectopic expression of ARHGDIB reduced the activated fractions of RhoA and Rac1 to 4.1% and 3.6%, respectively (Fig. 2B and C). Similar observations were made for MT-4 and SUP-T1 cells (data not shown).

These observations clearly indicated that ARHGDIB attenuates RhoA and Rac1 activity simultaneously in these T cell lines and suggested that RhoA and Rac1 are the primary targets of ectopically expressed ARHGDIB. Note that RhoA and Rac1 levels were increased by 1.4- and 1.3-fold, respectively, in cells ectopically expressing ARHGDIB, according to the densitometric analysis (Fig. 2B and C). This is due to the ARHGDIB-mediated stabilization of Rho GTPases, as

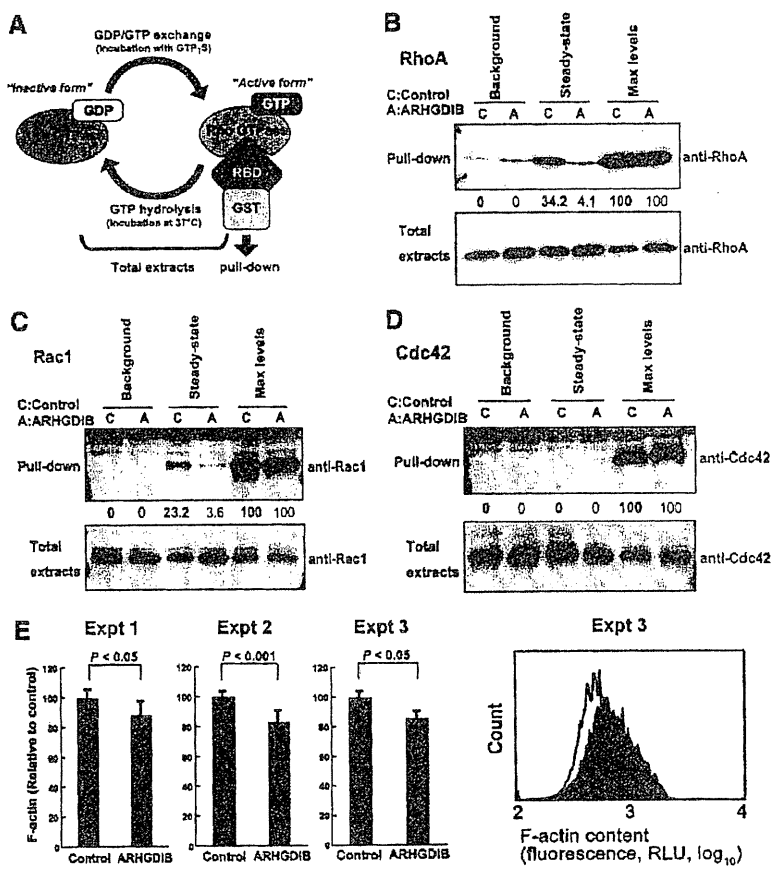


FIG. 2. Activation of RhoA and Rac1 under steady-state conditions in PM1 cells. (A) The experimental procedure for the active Rho GTPase capture assay. The active GTP-bound form is collected by glutathione-Sepharose beads coated with an RBD-GST fusion protein and compared with the total expression levels of each Rho GTPase by Western blot analysis. Incubation of the cell lysate with GTPγS shifts the equilibrium to the right, and incubation of the cell lysate at 37°C for 30 min shifts it to the left, representing the maximal activation levels (Max levels in B–D) or the background levels (background in B–D) of each Rho GTPase, respectively. (B–D) Activation of RhoA (B), Rac1 (C), and Cdc42 (D) in PM1 cells. The activation levels under steady-state conditions were estimated by densitometric analysis defined by setting the Max levels and background to 100% and 0%, respectively. (E) Measurement of F-actin content in PM1/ARHGDIB and control cells. Data from three independent experiments are shown in the bar graphs, and each of these experiments was performed in triplicate. The right panel shows the flow cytometric profile of Experiment 3, in which PM1/ARHGDIB is indicated by a black line, and the control is shown in gray. Statistical significance between the two groups was analyzed by two-tailed Student's *t*-test. AU, arbitrary unit.

reported previously.[31] This effect is modest in Cdc42 (1.1-fold, Fig. 2D) because the capture of Rho GTPase by ARHGDIB depends on the active GDP/GTP exchange cycle of Rho GTPase under steady-state conditions, which occurs inefficiently in Cdc42.

The common effector function of RhoA and Rac1 is the reorganization of the actin cytoskeleton.[11,12,32,33] If the ectopic expression of ARHGDIB inhibits RhoA and Rac1 effector function, the monomer-polymer actin equilibrium in ARHGDIB-transduced cells should be shifted toward a depolymerized state.[13,14,34] To test this, flow cytometry using fluorescently labeled phalloidin, which binds to F-actin, was used to measure the amount of polymerized actin. Under steady-state conditions, the fluorescence intensity of PM1/ARHGDIB cells was significantly lower than in control cells (Fig. 2E). The reduction levels of F-actin content in PM1/ARHGDIB cells were 14.2 ± 1.6% ($N=3$, $p<0.05$ by Student's $t$-test, two-tailed; Fig. 2E) compared with the control. A similar trend was observed in SUP-T1 cells. These data are in agreement with the results obtained by the active Rho GTPase capture assay and the previous findings that the overexpression of RhoGDI in various cell lines induces the disruption of actin cytoskeleton-dependent processes.[35–37] These data indicate that the ectopic expression of ARHGDIB in T cells suppresses the activation status of both RhoA and Rac1 under steady-state tissue culture conditions.

### *Analysis of the viral life cycle in ARHGDIB-expressing T cells*

Next, the mechanism by which ARHGDIB blocks HIV-1 replication was investigated. To do this, the viral entry and production phases were examined separately.

To examine the viral entry phase, PM1/ARHGDIB cells were infected with X4-tropic HIV-$1_{NL4-3}$ Env- or VSV-G-pseudotyped HIV-1 that produces luciferase upon the establishment of infection. In these viruses, luciferase is under the regulation of a long terminal repeat (LTR) or cytomegalovirus (CMV) promoter. When the relative luciferase activity in the control cells was set at 100%, the infection efficiency of HIV-1 Env-pseudotyped HIV-1 expressing luciferase driven by the HIV-1 LTR promoter was 33.0 ± 2.6% ($N=3$, $p<0.001$ by Student's $t$-test, two-tailed; Fig. 3A). Similar results were observed in MT-4 cells (data not shown). In contrast, the infection efficiency of VSV-G-pseudotyped HIV-1 expressing luciferase with either the HIV-1 LTR or CMV promoter was 243.2 ± 31.9% ($N=3$, $p<0.01$; Fig. 3A) or 480.3 ± 158.1% ($N=3$, $p<0.05$; Fig. 3A), respectively. Similarly, infection with VSV-G-pseudotyped MLV driving the expression of luciferase with the MLV LTR promoter was 10.0 ± 6.4-fold more efficient in PM1/ARHGDIB than in control cells ($N=4$, $p<0.05$; Fig. 3A). To examine the effect of ARHGDIB on gene expression, reporter plasmids driving the expression of luciferase with either the CMV or HIV-1 LTR promoter were transfected into PM1 cells. The LTR- and CMV-driven luciferase activities in PM1/ARHGDIB cells were modestly increased compared with the control cells, but not decreased (2.1 ± 0.6-fold, and 2.4 ± 1.6-fold for LTR- and CMV-driven constructs, six and four independent experiments, respectively; Fig. 3B). Taken together, these data suggest that the inhibition of viral entry is specific to HIV-1 Env, and the early phase of the viral life cycle is strongly affected.

When measured by flow cytometry, PM1/ARHGDIB cells were found to express cell surface CD4 at levels 1.4-fold higher than control cells (average of four independent experiments), while the cell surface levels of CXCR4 were 0.8-fold higher (average of five independent experiments). Considering that ARHGDIB did not affect the levels of cell surface CD4 or CXCR4 in MT-4 cells (Fig. 1B) and M8166 cells (data not shown), and that the reduction in CXCR4 expression in PM1 cells is relatively modest, these data suggest that changes in the expression of viral receptors do not fully account per se for the decreased susceptibility of PM1/ARHGDIB cells to HIV-$1_{NL4-3}$ Env-pseudotyped HIV-1.

To examine the production phase, proviral DNA was transfected into PM1/ARHGDIB and the control cells, and the viral protein expression in cells and the level of viral production in the culture supernatant were measured. The transfected cells were cultured in the presence of the antiretroviral drug efavirenz, which inhibits the replication cycle of HIV-1, allowing the assessment of viral production in the transfected cells. The levels of viral Gag in PM1/ARHGDIB cells, which are cleaved by protease to yield multiple bands in Western blot analysis with an anti-$p24^{CA}$ antibody, were comparable to the control cells (Fig. 3C). To assess these data quantitatively, densitometric analysis was conducted to quantify the signals representing $Pr55^{Gag}$, MA-CA, and $p24^{CA}$. Then, the percentage of $p24^{CA}$ and MA-CA relative to the total signal was calculated; this represented the efficiency of Gag processing. The Gag processing efficiency was 75.5% in PM1/ARHGDIB cells, similar to the control cells (69.9%). In addition, the ratio of the total signal in the viral lysate to that in the cell lysate was calculated. This reflects the efficiency of viral production. The virus/cell intensity ratios were 0.43 and 0.56 for the controls and cells ectopically expressing ARHGDIB, respectively. Similar data were obtained in an independent experiment in PM1 cells. These data suggest that the negative effect of ARHGDIB on the viral production phase was undetectable in T cells.

A single-round HIV-1 infection experiment was performed in the presence of a specific ROCK inhibitor, Y27632, to test whether the effector functions of RhoA are critical in regulating HIV-1 infection. The inhibition of ROCK, a RhoA signal mediator, reduced HIV-1 infection by 48.6 ± 6.3% compared with the control levels ($N=4$, $p<0.05$ by Student's $t$-test, two-tailed; Fig. 3D). These observations suggested that the RhoA signal triggered by HIV-1 Env-receptor interaction is involved in the regulation of HIV-1 infection. This inhibition of ROCK accounted for approximately 77% of the inhibition of HIV-1 infection in PM1 cells ectopically expressing ARHGDIB (33.0% vs. 48.6%; Fig. 3A and D). These data also suggested that Rac1 plays a supplementary role in the restriction of HIV-1 infection. Taken together, this suggests that ARHGDIB limits HIV-1 replication primarily by affecting Env-mediated processes, most likely via receptor clustering and virus-cell membrane fusion.

## Discussion

A handful of lymphoid-specific cellular regulators of HIV-1 replication are known, including CD4 and CCR5. However, few hematopoietic lineage-specific inhibitors of HIV-1 replication have been identified. Recently a dendritic- and myeloid-cell-specific restriction factor SAMHD1 has been

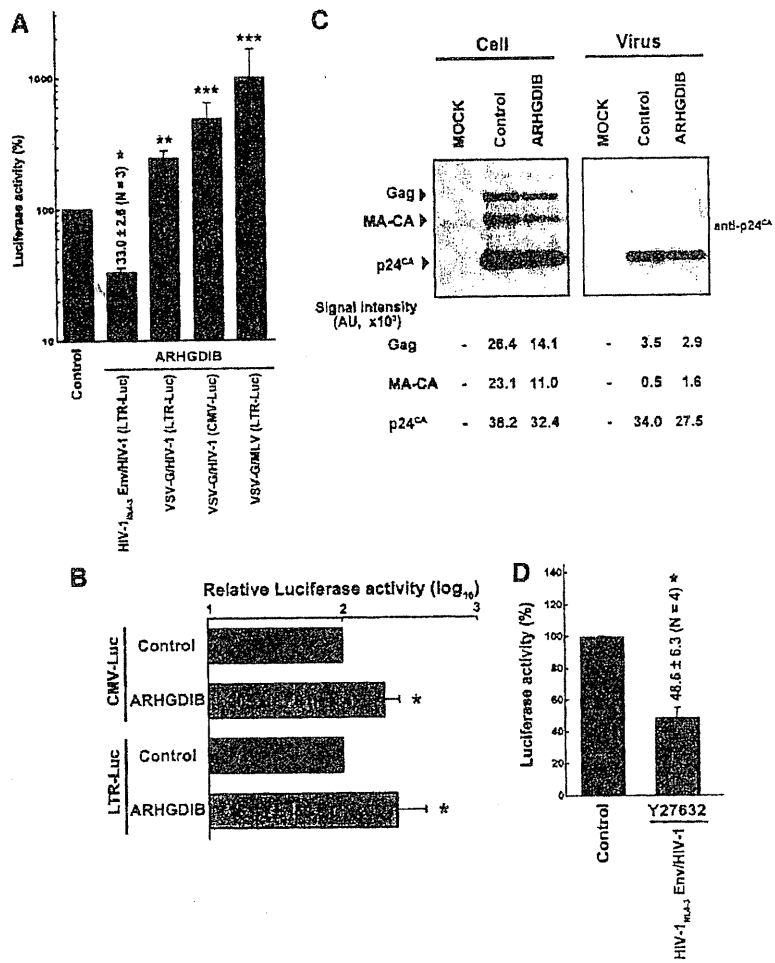


FIG. 3. The effect of ARHGDIB expression on the HIV-1 life cycle. (**A**) Single-round infection assay using replication-incompetent HIV-1 and MLV expressing luciferase upon integration, pseudotyped either with HIV-1 Env or with VSV-G. The promoters driving the expression of luciferase are noted in parentheses. Luciferase signals detected in PM1/ARHGDIB cells (gray) relative to control cells (black) are shown. The data represent the average and standard deviation from three or four independent experiments. Statistical significance between each group and the control was analyzed by two-tailed Student's *t*-test (single asterisk, $p < 0.001$; double asterisk, $p < 0.01$; and triple asterisk, $p < 0.05$). (**B**) Transient transfection assay to assess the effect of ARHGDIB on reporter gene expression. CMV- or HIV-1 LTR-driven luciferase expression vectors were introduced into PM1/control or PM1/ARHGDIB cells. Luciferase signals detected in PM1/ARHGDIB cells (gray) relative to control cells (black) are shown. The average and standard deviation from four and six independent experiments for CMV and LTR constructs, respectively, are shown. Statistical significance between PM1/ARHGDIB and the control was analyzed by two-tailed Student's *t*-test (asterisk, $p < 0.05$). (**C**) Viral production was assessed by transfecting proviral DNA into PM1/ARHGDIB and control cells. Viral protein levels in the cell lysate (Cell) and the pellet from the culture supernatant (Virus) were measured by Western blot analysis using anti-$p24^{CA}$ monoclonal antibody. The expression levels of Gag, MA-CA and $p24^{CA}$ were assessed by densitometric analysis and are shown in the lower panel. (**D**) Single-round infection assay in the presence of a ROCK inhibitor, Y27632. Luciferase signals detected in PM1/ARHGDIB cells (gray) relative to control cells (black) are shown. The data represent the average and standard deviation from four independent experiments. Statistical significance between each group and the control was analyzed by two-tailed Student's *t*-test (asterisk, $p < 0.05$).

reported.[38] APOBEC3 family members, which exhibit antiretroviral activity, may be hematopoietic cell specific, although their expression levels in non-T cells have not been directly examined.[39,40] In this study, we showed that modest up-regulation of the hematopoietic cell-specific RhoGDI, ARHGDIB, negatively regulated HIV-1 replication in various T cell lines, while it appeared to have no impact on cell proliferation. ARHGDIB is a constitutively expressed, lymphoid-specific protein. Therefore, ARHGDIB could provide intrinsic immunity against HIV-1 infection. In contrast, APOBEC3 family members are primarily interferon inducible.

RhoGDIs have not been isolated as negative regulators of HIV-1 replication in previous genetic screening studies. This is partly because nonlymphoid cells were used to screen genetic materials and the siRNA/shRNA-based gene knockdown is not able to identify negative regulators of HIV-1 replication at high sensitivity. Moreover, previous screens could not identify all potential factors, especially those present in the hematopoietic cell lineage, since nonlymphoid cells were often used. Our T cell-based screen using replication-competent HIV-1 allowed us to identify ARHGDIB as an HIV-1 inhibitor.

Rho GTPases play multiple roles in cell biology, including actin reorganization, endocytosis, and tubulin regulation, and ARHGDIB is a negative regulator of Rho GTPases.[11–14,32,41,42] It has been reported previously that inhibition of RhoA affects

viral receptor clustering, which lowers the efficiency of virus-cell membrane fusion and thus affects viral replication.[4,43–45] In contrast, the Rac1-PAK pathway has been shown to support virus-cell membrane fusion.[46,47] Both processes require active actin reorganization.[4,42,44–47] Interestingly, HIV-1 Env-guided entry is supported by a Filamin A-RhoA-ROCK axis and Arp2/3 complex, both of which are commonly involved in actin cytoskeletal reorganization.[21,44] Our data link the reported functions of RhoA, Rac1, and RhoGDIs with the biological phenotype of ARHGDIB; inhibition of HIV-1 replication in T cells. This HIV-1 inhibitory function of ARHGDIB is exerted via simultaneous functional restriction of two Rho GTPases, RhoA and Rac1. It is likely that receptor clustering and virus-cell membrane fusion are affected in T cells ectopically overexpressing ARHGDIB. As receptor clustering is the initial event of the HIV-1 life cycle, HIV-1 replication is attenuated in such cells regardless of the route of HIV-1 entry. Also, in T cells ectopically overexpressing ARHGDIB, RhoA and Rac1 are substantially inactivated. However, they are not inactivated completely. Thus, these cells are still able to support HIV-1 replication at certain levels, contributing to the delayed HIV-1 replication phenotype in cells ectopically overexpressing ARHGDIB.

Some reports suggest that RhoA inhibits LTR-mediated transcription.[43,48,49] If this is the case, increased ARHGDIB expression should enhance LTR-mediated transcription. In PM1/ARHGDIB cells, HIV-1 LTR-driven luciferase activity was slightly enhanced (Fig. 3B), which is consistent with previously reported findings. On the other hand, HIV-1 replication was repressed in T cells, suggesting that this transcriptional effect on viral replication is modest, if it occurs at all. It is also possible that the enhancement of the luciferase signal may be due to increased endocytic activity in PM1/ARHGDIB cells, since the DEAE-Dextran protocol was employed for transfection, and similar levels of enhancement of CMV-driven transcription were observed in PM1/ARHGDIB cells as well.

Infection with VSV-G-pseudotyped HIV-1 and MLV, which enter cells via endocytosis accompanied by the rearrangement of actin filaments, is augmented in PM1/ARHGDIB cells (Fig. 3A). These findings are consistent with a previous report demonstrating that ARHGDIB stimulates endocytosis in cells with a lymphoid background.[50] The efficiency of VSV-G-pseudotyped MLV infection into PM1/ARHGDIB cells was higher than VSV-G-pseudotyped HIV-1. During the entry phase, HIV-1 utilizes microtubules to traffic toward the nucleus, whereas MLV does not seem to actively do so.[51,52] As ARHGDIB potentially inhibits Rho GTPases, thereby disturbing microtubular organization, it is possible that HIV-1 infection is blocked by ARHGDIB at the microtubule-dependent transport phase in addition to the receptor clustering phase. Alternatively, the relatively high infectious titers produced by the MLV vector may be responsible for the observed phenotype.

Our findings do not negate the possibility that ARHGDIB limits HIV-1 replication by restricting the functions of other effector molecules. For instance, ARHGDIB has also been shown to bind the RhoGEF protein Vav1 and the cytoskeletal protein ezrin, both of which have been implicated in the positive regulation of HIV-1 replication.[53–57] Thus, these factors may also contribute to the ARHGDIB-mediated inhibition of HIV-1 replication.

The treatment efficacy of HIV-1/AIDS by antiretroviral drugs has greatly improved. However, the adverse effects of antiretroviral drugs lower the quality of life of HIV-1-infected individuals, and the emergence of drug-resistant strains is anticipated for all of the currently available antiretroviral drugs. Insights into HIV-1-host interaction, such as that provided in this study, will aid in the design of novel antiretroviral drugs. Our findings may contribute not only to antiretroviral drug development but also to our understanding of viral pathogenesis. Considering the observation that a modest increase in ARHGDIB expression resulted in the inhibition of HIV-1 replication, it is possible that, at the later phase of HIV-1 infection, CD4-positive cells bearing higher levels of ARHGDIB may be selected. Thus, ARHGDIB levels may be useful as a progression marker of HIV-1 infection. HIV-1 disease progression may be delayed in individuals who have relatively high levels of ARHGDIB in CD4-positive T cells. These possibilities should be examined in future studies.

## Acknowledgments

This work was supported in part by the Japan Human Science Foundation, the Japanese Ministry of Health, Labor and Welfare (Research on HIV/AIDS), and the Japanese Ministry of Education, Culture, Sports, Science and Technology (Priority Areas "Matrix of Infection Phenomena" 18073008).

## Author Disclosure Statement

No competing financial interests exist.

## References

1. Lu X, Wu X, Plemenitas A, *et al.*: CDC42 and Rac1 are implicated in the activation of the Nef-associated kinase and replication of HIV-1. Curr Biol 1996;6(12):1677–1684.
2. Cook JA, Albacker L, August A, and Henderson AJ: CD28-dependent HIV-1 transcription is associated with Vav, Rac, and NF-kappa B activation. J Biol Chem 2003;278(37):35812–35818.
3. Akasaki T, Koga H, and Sumimoto H: Phosphoinositide 3-kinase-dependent and -independent activation of the small GTPase Rac2 in human neutrophils. J Biol Chem 1999; 274(25):18055–18059.
4. del Real G, Jimenez-Baranda S, Mira E, *et al.*: Statins inhibit HIV-1 infection by down-regulating Rho activity. J Exp Med 2004;200(4):541–547.
5. Loomis RJ, Holmes DA, Elms A, Solski PA, Der CJ, and Su L: Citron kinase, a RhoA effector, enhances HIV-1 virion production by modulating exocytosis. Traffic 2006;7(12):1643–1653.
6. Pontow S, Harmon B, Campbell N, and Ratner L: Antiviral activity of a Rac GEF inhibitor characterized with a sensitive HIV/SIV fusion assay. Virology 2007;368(1):1–6.
7. Galandrini R, Henning SW, and Cantrell DA: Different functions of the GTPase Rho in prothymocytes and late pre-T cells. Immunity 1997;7(1):163–174.
8. Brown A, Wang X, Sawai E, and Cheng-Mayer C: Activation of the PAK-related kinase by human immunodeficiency virus type 1 Nef in primary human peripheral blood lymphocytes and macrophages leads to phosphorylation of a PIX-p95 complex. J Virol 1999;73(12):9899–9907.

9. Zhang B, Zhang Y, Dagher MC, and Shacter E: Rho GDP dissociation inhibitor protects cancer cells against drug-induced apoptosis. Cancer Res 2005;65(14):6054–6062.
10. Kolesnitchenko V, King L, Riva A, Tani Y, Korsmeyer SJ, and Cohen DI: A major human immunodeficiency virus type 1-initiated killing pathway distinct from apoptosis. J Virol 1997;71(12):9753–9763.
11. DerMardirossian C and Bokoch GM: GDIs: Central regulatory molecules in Rho GTPase activation. Trends Cell Biol 2005;15(7):356–363.
12. Dovas A and Couchman JR: RhoGDI: Multiple functions in the regulation of Rho family GTPase activities. Biochem J 2005;390(Pt 1):1–9.
13. Heasman SJ and Ridley AJ: Mammalian Rho GTPases: New insights into their functions from in vivo studies. Nat Rev Mol Cell Biol 2008;9(9):690–701.
14. Ladwein M and Rottner K: On the Rho'd: The regulation of membrane protrusions by Rho-GTPases. FEBS Lett 2008;582(14):2066–2074.
15. Brass AL, Dykxhoorn DM, Benita Y, *et al.*: Identification of host proteins required for HIV infection through a functional genomic screen. Science 2008;319(5865):921–926.
16. Zhou H, Xu M, Huang Q, *et al.*: Genome-scale RNAi screen for host factors required for HIV replication. Cell Host Microbe 2008;4(5):495–504.
17. Simmons A, Gangadharan B, Hodges A, *et al.*: Nef-mediated lipid raft exclusion of UbcH7 inhibits Cbl activity in T cells to positively regulate signaling. Immunity 2005;23(6):621–634.
18. Hodges A, Sharrocks K, Edelmann M, *et al.*: Activation of the lectin DC-SIGN induces an immature dendritic cell phenotype triggering Rho-GTPase activity required for HIV-1 replication. Nat Immunol 2007;8(6):569–577.
19. Urano E, Ichikawa R, Morikawa Y, Yoshida T, Koyanagi Y, and Komano J: T cell-based functional cDNA library screening identified SEC14-like 1a carboxy-terminal domain as a negative regulator of human immunodeficiency virus replication. Vaccine 2010;28(Suppl 2):B68–B74.
20. Urano E, Kariya Y, Futahashi Y, *et al.*: Identification of the P-TEFb complex-interacting domain of Brd4 as an inhibitor of HIV-1 replication by functional cDNA library screening in MT-4 cells. FEBS Lett 2008;582(29):4053–4058.
21. Komano J, Miyauchi K, Matsuda Z, and Yamamoto N: Inhibiting the Arp2/3 complex limits infection of both intracellular mature vaccinia virus and primate lentiviruses. Mol Biol Cell 2004;15(12):5197–5207.
22. Kimura K, Tsuji T, Takada Y, Miki T, and Narumiya S: Accumulation of GTP-bound RhoA during cytokinesis and a critical role of ECT2 in this accumulation. J Biol Chem 2000;275(23):17233–17236.
23. Takahashi Y, Tanaka Y, Yamashita A, Koyanagi Y, Nakamura M, and Yamamoto N: OX40 stimulation by gp34/OX40 ligand enhances productive human immunodeficiency virus type 1 infection. J Virol 2001;75(15):6748–6757.
24. Vicente-Manzanares M, Viton M, and Sanchez-Madrid F: Measurement of the levels of polymerized actin (F-actin) in chemokine-stimulated lymphocytes and GFP-coupled cDNA transfected lymphoid cells by flow cytometry. Methods Mol Biol 2004;239:53–68.
25. Shimizu S, Urano E, Futahashi Y, *et al.*: Inhibiting lentiviral replication by HEXIM1, a cellular negative regulator of the CDK9/cyclin T complex. AIDS 2007;21(5):575–582.
26. Sato K, Aoki J, Misawa N, *et al.*: Modulation of human immunodeficiency virus type 1 infectivity through incorporation of tetraspanin proteins. J Virol 2008;82(2):1021–1033.
27. Togawa A, Miyoshi J, Ishizaki H, *et al.*: Progressive impairment of kidneys and reproductive organs in mice lacking Rho GDIalpha. Oncogene 1999;18(39):5373–5380.
28. Reif K and Cantrell DA: Networking Rho family GTPases in lymphocytes. Immunity 1998;8(4):395–401.
29. Tuosto L, Michel F, and Acuto O: p95vav associates with tyrosine-phosphorylated SLP-76 in antigen-stimulated T cells. J Exp Med 1996;184(3):1161–1166.
30. Stowers L, Yelon D, Berg LJ, and Chant J: Regulation of the polarization of T cells toward antigen-presenting cells by Ras-related GTPase CDC42. Proc Natl Acad Sci USA 1995;92(11):5027–5031.
31. Boulter E, Garcia-Mata R, Guilluy C, *et al.*: Regulation of Rho GTPase crosstalk, degradation and activity by RhoGDI1. Nat Cell Biol 2010;12(5):477–483.
32. Etienne-Manneville S and Hall A: Rho GTPases in cell biology. Nature 2002;420(6916):629–635.
33. Dransart E, Morin A, Cherfils J, and Olofsson B: RhoGDI-3, a promising system to investigate the regulatory function of rhoGDIs: uncoupling of inhibitory and shuttling functions of rhoGDIs. Biochem Soc Trans 2005;33(Pt 4):623–626.
34. Lee SH and Dominguez R: Regulation of actin cytoskeleton dynamics in cells. Mol Cells 2010;29(4):311–325.
35. Takaishi K, Kikuchi A, Kuroda S, Kotani K, Sasaki T, and Takai Y: Involvement of rho p21 and its inhibitory GDP/GTP exchange protein (rho GDI) in cell motility. Mol Cell Biol 1993;13(1):72–79.
36. Miura Y, Kikuchi A, Musha T, *et al.*: Regulation of morphology by rho p21 and its inhibitory GDP/GTP exchange protein (rho GDI) in Swiss 3T3 cells. J Biol Chem 1993;268(1):510–515.
37. Komuro R, Sasaki T, Takaishi K, Orita S, and Takai Y: Involvement of Rho and Rac small G proteins and Rho GDI in Ca2+-dependent exocytosis from PC12 cells. Genes Cells 1996;1(10):943–951.
38. Laguette N, Sobhian B, Casartelli N, *et al.*: SAMHD1 is the dendritic- and myeloid-cell-specific HIV-1 restriction factor counteracted by Vpx. Retrovirology 2011;474(7353):654–657.
39. Koning FA, Newman EN, Kim EY, Kunstman KJ, Wolinsky SM, and Malim MH: Defining APOBEC3 expression patterns in human tissues and hematopoietic cell subsets. J Virol 2009;83(18):9474–9485.
40. Refsland EW, Stenglein MD, Shindo K, Albin JS, Brown WL, and Harris RS: Quantitative profiling of the full APOBEC3 mRNA repertoire in lymphocytes and tissues: Implications for HIV-1 restriction. Nucleic Acids Res 2010;38(13):4274–4284.
41. Ridley AJ: Rho GTPases and cell migration. J Cell Sci 2001;114(Pt 15):2713–2722.
42. Fukata M, Nakagawa M, and Kaibuchi K: Roles of Rho-family GTPases in cell polarisation and directional migration. Curr Opin Cell Biol 2003;15(5):590–597.
43. Iyengar S, Hildreth JE, and Schwartz DH: Actin-dependent receptor colocalization required for human immunodeficiency virus entry into host cells. J Virol 1998;72(6):5251–5255.
44. Jimenez-Baranda S, Gomez-Mouton C, Rojas A, *et al.*: Filamin-A regulates actin-dependent clustering of HIV receptors. Nat Cell Biol 2007;9(7):838–846.
45. Malinowsky K, Luksza J, and Dittmar MT: Susceptibility to virus-cell fusion at the plasma membrane is reduced through expression of HIV gp41 cytoplasmic domains. Virology 2008;376(1):69–78.
46. Pontow SE, Heyden NV, Wei S, and Ratner L: Actin cytoskeletal reorganizations and coreceptor-mediated activation

of rac during human immunodeficiency virus-induced cell fusion. J Virol 2004;78(13):7138–7147.
47. Harmon B and Ratner L: Induction of the Galpha(q) signaling cascade by the human immunodeficiency virus envelope is required for virus entry. J Virol 2008;82(18):9191–9205.
48. Wang L, Zhang H, Solski PA, Hart MJ, Der CJ, and Su L: Modulation of HIV-1 replication by a novel RhoA effector activity. J Immunol 2000;164(10):5369–5374.
49. Helms WS, Jeffrey JL, Holmes DA, Townsend MB, Clipstone NA, and Su L: Modulation of NFAT-dependent gene expression by the RhoA signaling pathway in T cells. J Leukoc Biol 2007;82(2):361–369.
50. Lamaze C, Chuang TH, Terlecky LJ, Bokoch GM, and Schmid SL: Regulation of receptor-mediated endocytosis by Rho and Rac. Nature 1996;382(6587):177–179.
51. Sodeik B: Unchain my heart, baby let me go—the entry and intracellular transport of HIV. J Cell Biol 2002;159(3):393–395.
52. Naghavi MH and Goff SP: Retroviral proteins that interact with the host cell cytoskeleton. Curr Opin Immunol 2007;19(4):402–407.
53. Haedicke J, de Los Santos K, Goff SP, and Naghavi MH: The Ezrin-radixin-moesin family member ezrin regulates stable microtubule formation and retroviral infection. J Virol 2008;82(9):4665–4670.
54. Hecker C, Weise C, Schneider-Schaulies J, Holmes HC, and ter Meulen V: Specific binding of HIV-1 envelope protein gp120 to the structural membrane proteins ezrin and moesin. Virus Res 1997;49(2):215–223.
55. Kubo Y, Yoshii H, Kamiyama H, *et al.*: Ezrin, Radixin, and Moesin (ERM) proteins function as pleiotropic regulators of human immunodeficiency virus type 1 infection. Virology 2008;375(1):130–140.
56. Barrero-Villar M, Cabrero JR, Gordon-Alonso M, *et al.*: Moesin is required for HIV-1-induced CD4-CXCR4 interaction, F-actin redistribution, membrane fusion and viral infection in lymphocytes. J Cell Sci 2009;122(Pt 1):103–113.
57. Fackler OT, Luo W, Geyer M, Alberts AS, and Peterlin BM: Activation of Vav by Nef induces cytoskeletal rearrangements and downstream effector functions. Mol Cell 1999; 3(6):729–739.

Address correspondence to:
*Jun Komano*
*AIDS Research Center*
*National Institute of Infectious Diseases*
*1-23-1 Toyama, Shinjuku*
*Tokyo 162-8640, Japan*

*E-mail:* ajkomano@nih.go.jp

# Novel Mouse Xenograft Models Reveal a Critical Role of CD4$^+$ T Cells in the Proliferation of EBV-Infected T and NK Cells

**Ken-Ichi Imadome[1☯*], Misako Yajima[1☯¤], Ayako Arai[2], Atsuko Nakazawa[3], Fuyuko Kawano[1], Sayumi Ichikawa[1,4], Norio Shimizu[4], Naoki Yamamoto[5¤], Tomohiro Morio[6], Shouichi Ohga[7], Hiroyuki Nakamura[1], Mamoru Ito[8], Osamu Miura[2], Jun Komano[5], Shigeyoshi Fujiwara[1*]**

**1** Department of Infectious Diseases, National Research Institute for Child Health and Development, Tokyo, Japan, **2** Department of Hematology, Tokyo Medical and Dental University, Tokyo, Japan, **3** Department of Pathology, National Center for Child Health and Development, Tokyo, Japan, **4** Department of Virology, Division of Medical Science, Medical Research Institute, Tokyo Medical and Dental University, Tokyo, Japan, **5** AIDS Research Center, National Institute of Infectious Diseases, Tokyo, Japan, **6** Department of Pediatrics and Developmental Biology, Tokyo Medical and Dental University, Tokyo, Japan, **7** Department of Perinatal and Pediatric Medicine, Graduate School of Medical Sciences, Kyushu University, Fukuoka, Japan, **8** Central Institute for Experimental Animals, Kawasaki, Japan

## Abstract

Epstein-Barr virus (EBV), a ubiquitous B-lymphotropic herpesvirus, ectopically infects T or NK cells to cause severe diseases of unknown pathogenesis, including chronic active EBV infection (CAEBV) and EBV-associated hemophagocytic lymphohistiocytosis (EBV-HLH). We developed xenograft models of CAEBV and EBV-HLH by transplanting patients' PBMC to immunodeficient mice of the NOD/Shi-*scid*/IL-2R$\gamma^{null}$ strain. In these models, EBV-infected T, NK, or B cells proliferated systemically and reproduced histological characteristics of the two diseases. Analysis of the TCR repertoire expression revealed that identical predominant EBV-infected T-cell clones proliferated in patients and corresponding mice transplanted with their PBMC. Expression of the EBV nuclear antigen 1 (EBNA1), the latent membrane protein 1 (LMP1), and LMP2, but not EBNA2, in the engrafted cells is consistent with the latency II program of EBV gene expression known in CAEBV. High levels of human cytokines, including IL-8, IFN-$\gamma$, and RANTES, were detected in the peripheral blood of the model mice, mirroring hypercytokinemia characteristic to both CAEBV and EBV-HLH. Transplantation of individual immunophenotypic subsets isolated from patients' PBMC as well as that of various combinations of these subsets revealed a critical role of CD4$^+$ T cells in the engraftment of EBV-infected T and NK cells. In accordance with this finding, in vivo depletion of CD4$^+$ T cells by the administration of the OKT4 antibody following transplantation of PBMC prevented the engraftment of EBV-infected T and NK cells. This is the first report of animal models of CAEBV and EBV-HLH that are expected to be useful tools in the development of novel therapeutic strategies for the treatment of the diseases.

**Citation:** Imadome K-I, Yajima M, Arai A, Nakazawa A, Kawano F, et al. (2011) Novel Mouse Xenograft Models Reveal a Critical Role of CD4$^+$ T Cells in the Proliferation of EBV-Infected T and NK Cells. PLoS Pathog 7(10): e1002326. doi:10.1371/journal.ppat.1002326

**Editor:** Shou-Jiang Gao, University of Texas Health Science Center San Antonio, United States of America

**Received** January 27, 2011; **Accepted** September 2, 2011; **Published** October 20, 2011



**Funding:** This study was supported by grants from the Ministry of Health, Labour and Welfare of Japan (H22-Nanchi-080 and H22-AIDS-002), the Grant of National Center for Child Health and Development (22A-9), a grant for the Research on Publicly Essential Drugs and Medical Devices from The Japan Health Sciences Foundation (KHC1014), and the Grant-in-Aid for Scientific Research (C) (H22-22590374). The funders had no role in study design, data collection and analysis, decision to publish, or preparation of the manuscript.

**Competing Interests:** The authors have declared that no competing interests exist.

* E-mail: imadome@nch.go.jp (KI); shige@nch.go.jp (SF)

¤ Current address: Department of Microbiology, Yong Loo Lin School of Medicine, National University of Singapore, Singapore

☯ These authors contributed equally to this work.

## Introduction

Epstein-Barr virus (EBV) is a ubiquitous $\gamma$-herpesvirus that infects more than 90% of the adult population in the world. EBV is occasionally involved in the pathogenesis of malignant tumors, such as Burkitt lymphoma, Hodgkin lymphoma, and nasopharyngeal carcinoma, along with the post-transplantation lymphoproliferative disorders in immunocompromised hosts. Although EBV infection is asymptomatic in most immunologically competent hosts, it sometimes causes infectious mononucleosis (IM), when primarily infecting adolescents and young adults [1]. EBV infects human B cells efficiently in vitro and transform them into lymphoblastoid cell lines (LCLs) [2]. Experimental infection of T and NK cells, in contrast, is practically impossible except in limited conditions [3,4]. Nevertheless, EBV has been consistently demonstrated in T or NK cells proliferating monoclonally or oligoclonally in a group of diseases including chronic active EBV infection (CAEBV) and EBV-associated hemophagocytic lymphohistiocytosis (EBV-HLH) [5,6,7,8,9,10]. CAEBV, largely overlapping the systemic EBV$^+$ T-cell lymphoproliferative diseases of childhood defined in the WHO classification of lymphomas [11], is characterized by prolonged or relapsing IM-like symptoms, unusual patterns of antibody responses to EBV, and elevated EBV DNA load in the peripheral blood [12,13,14]. CAEBV has a chronic time course with generally poor prognosis; without a proper treatment by hematopoietic stem cell transplantation, the

## Author Summary

Epstein-Barr virus (EBV) is a ubiquitous human herpesvirus that infects more than 90% of the adult human population in the world. EBV usually infects B lymphocytes and does not produce symptoms in infected individuals, but in rare occasions it infects T or NK lymphocytes and causes severe diseases such as chronic active EBV infection (CAEBV) and EBV-associated hemophagocytic lymphohistiocytosis (EBV-HLH). We developed mouse models of these two human diseases in which EBV-infected T or NK lymphocytes proliferate in mouse tissues and reproduce human pathologic conditions such as overproduction of small proteins called "cytokines" that produce inflammatory responses in the body. These mouse models are thought to be very useful for the elucidation of the pathogenesis of CAEBV and EBV-HLH as well as for the development of therapeutic strategies for the treatment of these diseases. Experiments with the models demonstrated that a subset of lymphocytes called CD4-positive lymphocytes are essential for the proliferation of EBV-infected T and NK cells. This result implies that removal of CD4-positive lymphocytes or suppression of their functions may be an effective strategy for the treatment of CAEBV and EBV-HLH.


majority of cases eventually develop malignant lymphoma of T or NK lineages, multi-organ failure, or other life-threatening conditions. Monoclonal or oligoclonal proliferation of EBV-infected T and NK cells, an essential feature of CAEBV, implies its malignant nature, but other characteristics of CAEBV do not necessarily support this notion. For example, EBV-infected T or NK cells freshly isolated from CAEBV patients, as well as established cell lines derived from them, do not have morphological atypia and do not engraft either in nude mice or *scid* mice (Shimizu, N., unpublished results). Clinically, CAEBV has a chronic time course and patients may live for many years without progression of the disease [15]. Although patients with CAEBV do not show signs of explicit immunodeficiency, some of them present a deficiency in NK-cell activity or in EBV-specific T-cell responses, implying a role for subtle immunodeficiency in its pathogenesis [16,17,18].

EBV-HLH is the most common and the severest type of virus-associated HLH and, similar to CAEBV, characterized by monoclonal or oligoclonal proliferation of EBV-infected T (most often $CD8^+$ T) cells [5,6]. Clinical features of EBV-HLH include high fever, pancytopenia, coagulation abnormalities, hepatosplenomegaly, liver dysfunction, and hemophagocytosis [19]. Overproduction of cytokines by EBV-infected T cells as well as by activated macrophages and T cells reacting to EBV is thought to play a central role in the pathogenesis [20]. Although EBV-HLH is an aggressive disease requiring intensive clinical interventions, it may be cured, in contrast to CAEBV, by proper treatment with immunomodulating drugs [21]. No appropriate animal models have been so far developed for either CAEBV or EBV-HLH.

NOD/Shi-*scid*/IL-2R$\gamma^{null}$ (referred here as NOG) is a highly immunodeficient mouse strain totally lacking T, B, and NK lymphocytes, and transplantation of human hematopoietic stem cells to NOG mice results in reconstitution of human immune system components, including T, B, NK cells, dendritic cells, and macrophages [22,23]. These so called humanized mice have been utilized as animal models for the infection of certain human viruses targeting the hemato-immune system, including human immunodeficiency virus 1 (HIV-1) and EBV [24,25,26,27,28,29,30]. Xenotransplantation of human tumor cells to NOG mice also provided model systems for several hematologic malignancies [31,32,33]. To facilitate investigations on the pathogenesis of CAEBV and EBV-HLH and assist the development of novel therapeutic strategies, we generated mouse models of these two EBV-associated diseases by transplanting NOG mice with PBMC isolated from patients with the diseases. In these models, EBV-infected T, NK, or B cells engrafted in NOG mice and reproduced lymphoproliferative disorder similar to either CAEBV or EBV-HLH. Further experiments with the models revealed a critical role of $CD4^+$ T cells in the in vivo proliferation of EBV-infected T and NK cells.

## Results

### Engraftment of EBV-infected T and NK cells in NOG mice following xenotransplantation with PBMC of CAEBV patients

Depending on the immunophenotypic subset in which EBV causes lymphoproliferation, CAEBV is classified into the T-cell and NK-cell types, with the former being further divided into the CD4, CD8, and γδT types. The nine patients with CAEBV examined in this study are characterized in Table 1 and include all these four types. Intravenous injection of $1-4\times10^6$ PBMC isolated from these nine patients resulted in successful engraftment of EBV-infected T or NK cells in NOG mice in a reproducible manner (Table 1). The results with the patient 1 (CD4 type), patient 3 (CD8 type), patient 5 (γδT type), and patient 9 (NK type) are shown in Figure 1. Seven to nine weeks post-transplantation, EBV DNA was detected in the peripheral blood of recipient mice and reached the levels of $10^5$–$10^8$ copies/μg DNA (Figure 1A). By contrast, no engraftment of EBV-infected cells was observed when immunophenotypic fractions containing EBV DNA were isolated from PBMC and injected to NOG mice (Figure 1A and Table 2). An exception was the $CD4^+$ T-cell fraction isolated from patients with the CD4 type CAEBV, that reproducibly engrafted when transplanted without other components of PBMC (Figure 1A, Table 2). Flow cytometry revealed that the major population of engrafted cells was either $CD4^+$, $CD8^+$, TCRγδor $CD16^+CD56^+$, depending on the type of the donor CAEBV patient (Figure 1B). EBV-infected cells of identical immunophenotypes were found in the patients and the corresponding mice that received their respective PBMC (Figure 1B). Although human cells of multiple immunophenotypes were present in most recipient mice, fractionation by magnetic beads-conjugated antibodies and subsequent real-time PCR analysis detected EBV DNA only in the predominant immunophenotypes that contained EBV DNA in the original patients (Figure 1B, Table 1). The EBV DNA load observed in individual lymphocyte subsets in the patient 3 and a mouse that received her PBMC is shown as supporting data (Table S1). When PBMC from three healthy EBV-carriers were injected intravenously to NOG mice, as controls, no EBV DNA was detected from either the peripheral blood, spleen, or liver (data not shown). Histological analyses of the spleen and the liver of these control mice identified no EBV-encoded small RNA (EBER)-positive cells, although some CD3-positive human T cells were observed (Figure S2). Analysis of TCR Vβ repertoire demonstrated an identical predominant T-cell clone in patients (patients 1 and 3) and the corresponding mice that received their PBMC (Figure 1C). The general condition of most recipient mice deteriorated gradually in the observation period of eight to twelve weeks, with loss of body weight (Figure S1), ruffled hair, and inactivity.

NOG mice engrafted with EBV-infected T or NK cells were sacrificed for pathological and virological analyses between eight

**Table 1.** Patients with EBV-T/NK LPD and the results of xenotransplantation of their PBMC to NOG mice.

| Patient number | Diagnosis | Sex | Age | Type of infected cells | [1]EBV DNA load in the patients | [2]Engrafted cells in mice | [3]Engraftment | [1]EBV DNA load in mice |
|---|---|---|---|---|---|---|---|---|
| 1 | CAEBV | F | 25 | CD4 | $9.2\times10^5$ | CD4, CD8 | 3/3 | $1.0\sim3.8\times10^7$ |
| 2 | CAEBV | M | 46 | CD4 | $1.3\sim7.2\times10^5$ | CD4, CD8 | 2/2, 3/3 | $2.6\sim10\times10^5$ |
| 3 | CAEBV | F | 35 | CD8 | $2.1\sim78\times10^5$ | CD8, CD4 | 2/2, 2/2 | $1.1\sim33\times10^6$ |
| 4 | CAEBV | M | 28 | CD8 | $8.2\times10^5$ | CD8, CD4 | 3/3 | $1.1\sim2.5\times10^6$ |
| 5 | CAEBV | M | 10 | γδT | $2.2\times10^6$ | γδT, CD4, CD8 | 2/2 | $3.8\sim6.5\times10^6$ |
| 6 | CAEBV | F | 15 | γδT | $6.2\times10^5$ | γδT, CD4, CD8 | 2/2 | $2.2\sim11\times10^5$ |
| 7 | CAEBV | M | 13 | NK | $1.1\sim6.7\times10^5$ | NK, CD4, CD8 | 2/2, 2/2 | $0.6\sim15\times10^4$ |
| 8 | CAEBV | F | 13 | NK | $6.3\times10^6$ | NK, CD4, CD8 | 3/3, 2/2 | $0.8\sim1.9\times10^5$ |
| 9 | CAEBV | M | 8 | NK | $1.2\sim8.7\times10^5$ | NK, CD4, CD8 | 2/2, 3/3 | $1.8\sim7.2\times10^5$ |
| 10 | EBV-HLH | M | 10 | CD8 | $2.8\sim38\times10^4$ | CD8, CD4 | 2/2, 2/2 | $6.5\sim9.9\times10^4$ |
| 11 | EBV-HLH | M | 50 | CD8 | $6.2\times10^5$ | CD8, CD4 | 4/4 | $7.0\sim45\times10^4$ |
| 12 | EBV-HLH | M | 1 | CD8 | $3.1\times10^5$ | CD8, CD4 | 2/2 | $6.0\sim9.1\times10^4$ |
| 13 | EBV-HLH | M | 64 | CD8 | $3.2\sim3.9\times10^5$ | CD8, CD4 | 2/2, 2/2 | $5.0\sim30\times10^5$ |

[1]EBV DNA copies/μg DNA in the peripheral blood.
[2]EBV DNA was detected only in the cells of the underlined subsets.
[3]Number of mice with successful engraftment per number of recipient mice is shown for each experiment.
doi:10.1371/journal.ppat.1002326.t001

and twelve weeks post-transplantation. On autopsy, the majority of mice presented with splenomegaly, with slight hepatomegaly in occasional cases (Figure 2A). Histopathological findings obtained from a representative mouse (recipient of PBMC from the patient 3 (CD8 type)) are shown in Figure 2B and reveal infiltration of human $CD3^+CD20^-$ cells to major organs, including the spleen, liver, lungs, kidneys, and small intestine. These cells were positive for both EBER and human CD45RO, indicating that they are EBV-infected human T cells (Figure 2B). In contrast, no EBV-infected T cells were found in mice transplanted with PBMC isolated from a normal EBV carrier (Figure S2). Histopathology of a control NOG mouse is shown in Figure S2. Morphologically, EBV-infected cells are relatively small and do not have marked atypia. The infiltration pattern was leukemic and identical with chronic active EBV infection in children [34]. The architecture of the organs was well preserved in spite of marked lymphoid infiltration. The spleen showed marked expansion of periarterial lymphatic sheath owing to lymphocytic infiltration. In the liver, a dense lymphocytic infiltration was observed in the portal area and in the sinusoid. The lung showed a picture of interstitial pneumonitis and the lymphocytes often formed nodular aggregations around bronchioles and arteries. In the kidney, dense lymphocytic infiltration caused interstitial nephritis. In the small intestine, mild lymphoid infiltration was seen in mucosa. Quantification of EBV DNA in the spleen, liver, lymph nodes, lungs, kidneys, adrenals, and small intestine of this mouse revealed EBV DNA at the levels of $1.5–5.1\times10^7$ copies/μg DNA. Mice transplanted with PBMC derived from CAEBV of other types exhibited similar infiltration of EBV-infected T or NK cells to the spleen, liver, and other organs (Figure 2C and data not shown).

## EBV-infected T- and NK-cell lines established from CAEBV patients do not engraft in NOG mice

We established EBV-positive cell lines of $CD4^+$ T, $CD8^+$ T, γδT, and $CD56^+$ NK lineages from PBMC of the patients listed in Table 1 by the method described previously [35], and confirmed by flow cytometry that the surface phenotypes of EBV-infected cells in the original patients were retained in these cell lines (data not shown). To test whether these cell lines engraft in NOG mice, $1–4\times10^6$ cells were injected intravenously to NOG mice. The results are shown in Figure 3A and indicate that CAEBV-derived cell lines of the $CD8^+$ T, γδT, and $CD56^+$ NK phenotypes do not engraft in NOG mice. Neither human CD45-positive cells nor EBV DNA were detected in the peripheral blood of the mice up to twelve weeks post-transplantation. When the recipient mice were sacrificed at twelve weeks post-injection, no EBV DNA could be detected in the spleen, liver, bone marrow, mesenteric lymph nodes, and kidneys. In contrast, the $CD4^+$ T cell lines derived from the CD4-type patients 1 and 2 engrafted in NOG mice and induced T lymphoproliferation similar to that induced by PBMC isolated freshly from these patients (Figure 3A and data not shown). These results, together with the results of transplantation with EBV-containing subsets of PBMC, indicate that EBV-infected T and NK cells, with the exception of those of the $CD4^+$ subset, are not able to engraft in NOG mice, when they are separated from other components of PBMC, suggesting that some components of PBMC are essential for the outgrowth EBV-infected T and NK cells in NOG mice.

## Engraftment of EBV-infected T and NK cells in NOG mice requires $CD4^+$ T cells

To identify the cellular component required for the engraftment of EBV-infected T and NK cells in NOG mice, we transplanted PBMC of CAEBV patients after removing individual immunophenotypic subsets by magnetic beads-conjugated antibodies. The results are shown in Figure 3B and summarized in Table 2. With respect to the patients 3 and 4, in whom $CD8^+$ T cells are infected with EBV, removal of $CD8^+$ cells from PBMC, as expected, resulted in the failure of engraftment, whereas elimination of $CD19^+$, $CD56^+$, or $CD14^+$ cells did not affect engraftment. Importantly, elimination of $CD4^+$ cell fraction, that did not contain EBV DNA, resulted in the failure of engraftment of EBV-infected T cells (Figure 3B and data not shown). In the experiments with the patients 5 and 6, in whom γδT cells were infected, removal $CD4^+$ cells that did not contain EBV DNA, as well as that of γδT cells, resulted in the failure of engraftment.

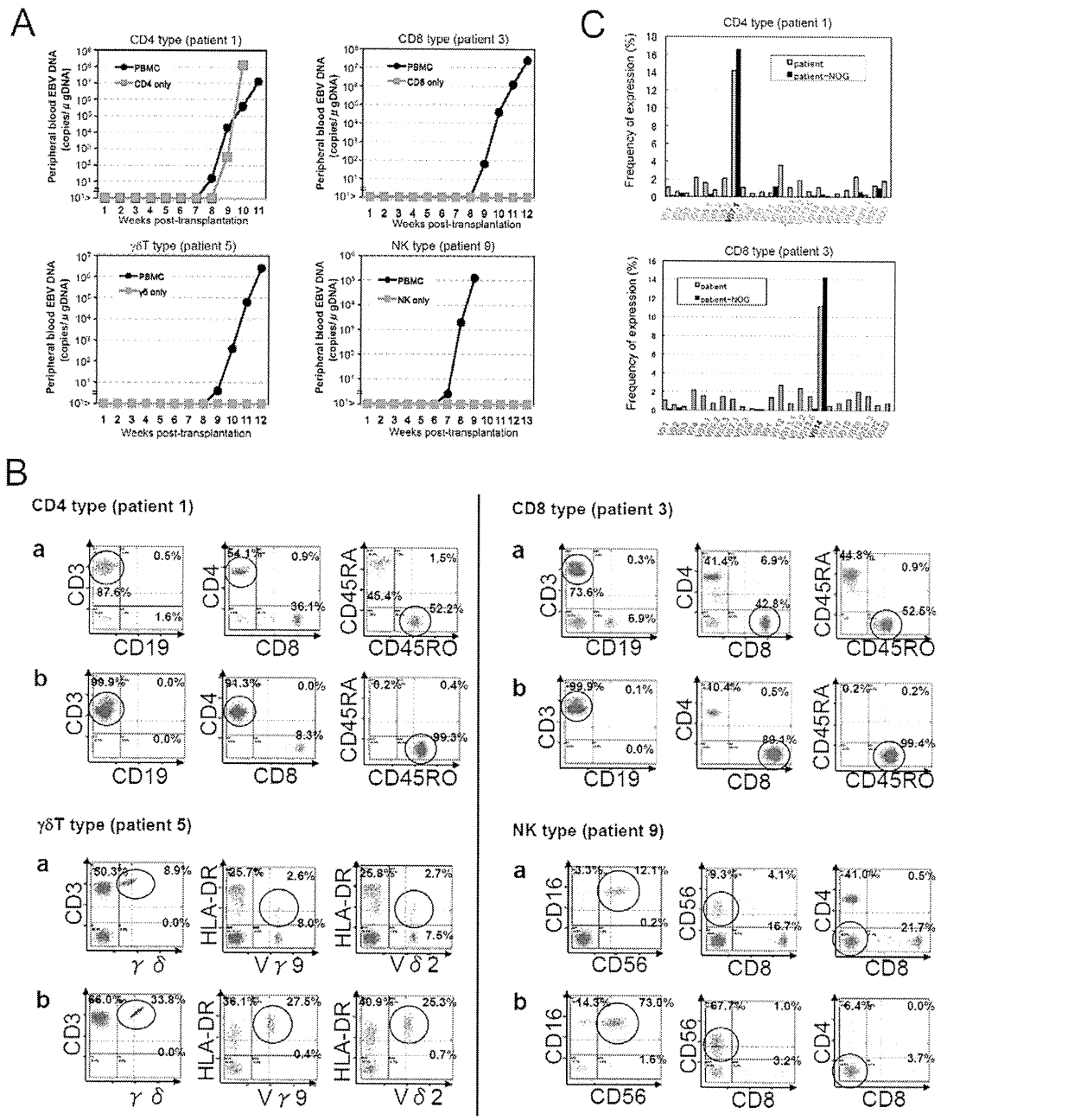


**Figure 1. Engraftment of EBV-infected T or NK cells in NOG mice following transplantation with PBMC of patients with CAEBV.** A. Measurement of EBV DNA levels. PBMC obtained from the CAEBV patients 1 (CD4 type), 3 (CD8 type), 5 (γδT type), and 9 (NK type) were injected intravenously to NOG mice and EBV DNA load in their peripheral blood was measured weekly by real-time PCR. The results of transplantation with whole PBMC or with isolated EBV DNA-containing cell fraction are shown. B. Flow-cytometric analysis on the expression of surface markers in the peripheral blood lymphocytes of patients (a) with CAEBV and NOG mice (b) that received PBMC from them. Human lymphocytes gated by the pattern of side scatter and human CD45 expression were further analyzed for the expression of various surface markers indicated in the figures. The results from the patients 1, 3, 5, and 9, and the corresponding mice that received their respective PBMC are shown. Circles indicate the fractions that contained EBV DNA. C. Analysis on the expression of TCR Vβ repertoire. Peripheral blood lymphocytes obtained from the patients 1 (CD4 type) and 3 (CD8 type), and from the corresponding mice that received their respective PBMC were analyzed for the expression of Vβ alleles. The percentages of T cells expressing each Vβ allele are shown for the patients (grey bars) and the mice (black bars).
doi:10.1371/journal.ppat.1002326.g001

Removal of $CD8^+$, $CD14^+$, $CD19^+$, or $CD56^+$ cells did not have an influence on the engraftment (Figure 3B and data not shown). Regarding the patients 8 an 9 in whom EBV resided in $CD56^+$ NK cells, removal of $CD4^+$ as well as $CD56^+$ cells resulted in the failure of engraftment, whereas that of $CD8^+$, $CD19^+$, or $CD14^+$ cells did not affect engraftment (Figure 3B and data not shown). In

**Table 2.** Results of xenotransplantation with subsets of PBMC obtained from CAEBV patients.

| Number of patient | Diagnosis | Phenotype of infected cells | Cell fraction transplanted | Number of transplanted cells | Engraftment |
|---|---|---|---|---|---|
| 1 | CAEBV | CD4 | PBMC | $2\times10^6$ | + |
| | | | CD4 | $2\times10^6$ | + |
| | | | PBMC-CD4 | $3\times10^6$ | − |
| | | | PBMC-CD8 | $2\times10^6$ | + |
| | | | PBMC-CD56 | $2\times10^6$ | + |
| | | | PBMC-CD14 | $2\times10^6$ | + |
| | | | PBMC-CD19 | $2\times10^6$ | + |
| 3 | CAEBV | CD8 | PBMC | $2\times10^6$ | + |
| | | | CD8 | $3\times10^6$ | − |
| | | | PBMC-CD4 | $3\times10^6$ | − |
| | | | PBMC-CD8 | $3\times10^6$ | − |
| | | | PBMC-CD56 | $2\times10^6$ | + |
| | | | PBMC-CD14 | $2\times10^6$ | + |
| | | | PBMC-CD19 | $2\times10^6$ | + |
| 5 | CAEBV | γδT | PBMC | $2\times10^6$ | + |
| | | | γδT | $3\times10^6$ | − |
| | | | PBMC-CD4 | $3\times10^6$ | − |
| | | | PBMC-γδT | $3\times10^6$ | − |
| | | | PBMC- CD8 | $3\times10^6$ | + |
| | | | PBMC-CD56 | $3\times10^6$ | + |
| | | | PBMC-CD14 | $3\times10^6$ | + |
| | | | PBMC-CD19 | $3\times10^6$ | + |
| 9 | CAEBV | NK | PBMC | $2\times10^6$ | + |
| | | | NK | $3\times10^6$ | − |
| | | | PBMC-CD4 | $3\times10^6$ | − |
| | | | PBMC-CD8 | $3\times10^6$ | + |
| | | | PBMC-CD56 | $3\times10^6$ | − |
| | | | PBMC-CD14 | $3\times10^6$ | + |
| | | | PBMC-CD19 | $3\times10^6$ | + |
| 11 | EBV-HLH | CD8 | PBMC | $2\times10^6$ | + |
| | | | PBMC-CD4 | $4\times10^6$ | − |

doi:10.1371/journal.ppat.1002326.t002

the patients 1 and 2, in whom $CD4^+$ T cells were infected, only the removal of $CD4^+$ cells blocked the engraftment of EBV-infected cells and depletion of either $CD8^+$, $CD19^+$, or $CD14^+$ cells had no effect (Figure 3B and data not shown). These results suggested that EBV-infected cells of the $CD8^+$, γδT, and $CD56^+$ lineages require $CD4^+$ cells for their engraftment in NOG mice. To confirm this interpretation, we performed complementation experiments, in which EBV-containing fractions of the $CD8^+$ (patient 4), γδT (patient 5), or $CD56^+$ (patient 7) phenotypes were transplanted together with autologous $CD4^+$ cells. The results are shown in Figure 3A and indicate that EBV-infected $CD8^+$, γδT, or $CD56^+$ cells engraft in NOG mice when transplanted together with $CD4^+$ cells. Similarly, when EBV-infected cell lines of the $CD8^+$, γδT, and $CD16^+$ lineages were injected intravenously to NOG mice together with autologous $CD4^+$ cells, these cell lines engrafted to the mice (Figure 3A). Finally, to further confirm the essential role of $CD4^+$ cells, we examined the effect of the OKT-4 antibody that depletes $CD4^+$ cells in vivo [24]. PBMC isolated from the CAEBV patient 3 (CD8 type) and the patient 8 (NK type) were injected intravenously to NOG mice and OKT-4 was administered intravenously for four consecutive days starting from the day of transplantation. The results are shown in Figure 4 and indicate that OKT-4 can strongly suppress the engraftment of EBV-infected T and NK cells. In the mice treated with OKT-4, no splenomegaly was observed and EBV DNA was not detected either in the peripheral blood, spleen, liver, or lungs at eight weeks post-transplantation.

## Analysis on the EBV gene expression associated with T or NK lymphoproliferation in NOG mice

Previous analysis of EBV gene expression in patients with CAEBV revealed the expression of EBNA1, LMP1, and LMP2A with the involvement of the Q promoter in the EBNA genes transcription and no expression of EBNA2, being consistent with the latency II type of EBV gene expression [36,37,38]. To test whether EBV-infected T and NK cells that proliferate in NOG mice retain this type of viral gene expression, we performed RT-PCR analysis in the spleen and the liver of mice that received

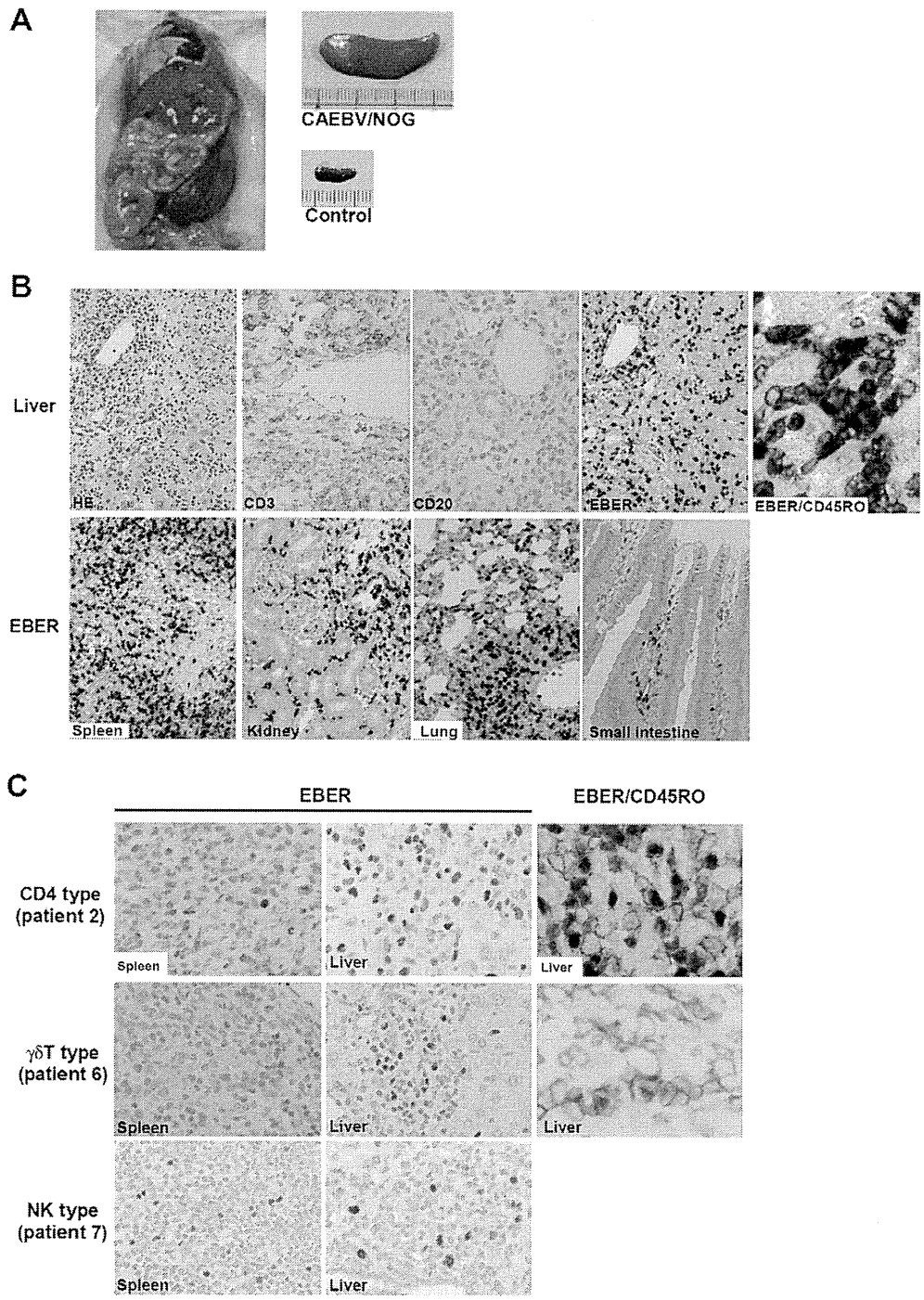


**Figure 2. Pathological and immunochemical analyses on NOG mice transplanted with PBMC from CAEBV patients.** A. Photographs of a model mouse showing splenomegaly and of the excised spleen. This mouse was transplanted with PBMC from the CAEBV patient 3 (CD8 type). Spleen from a control NOG mouse is also shown. B. Photomicrographs of various tissues of a mouse that received PBMC from the patient 3 (CD8 type). Upper panels: liver tissue was stained with hematoxylin-eosin (HE), antibodies specific to human CD3 or CD20, or by ISH with an EBER probe; the rightmost panel is a double staining with EBER and human CD45RO. Bottom panels: EBER ISH in the spleen, kidney, lung, and small intestine. Original magnification is ×200, except for EBER/CD45RO, that is ×400. C. Photomicrographs of the spleen and liver tissues obtained from NOG mice transplanted with PBMC from the CAEBV patients 2 (CD4 type), 6 (γδT type) or 7 (NK type). Tissues were stained by EBER-ISH or by double staining with EBER-ISH and human CD45RO. Original magnification ×600.
doi:10.1371/journal.ppat.1002326.g002

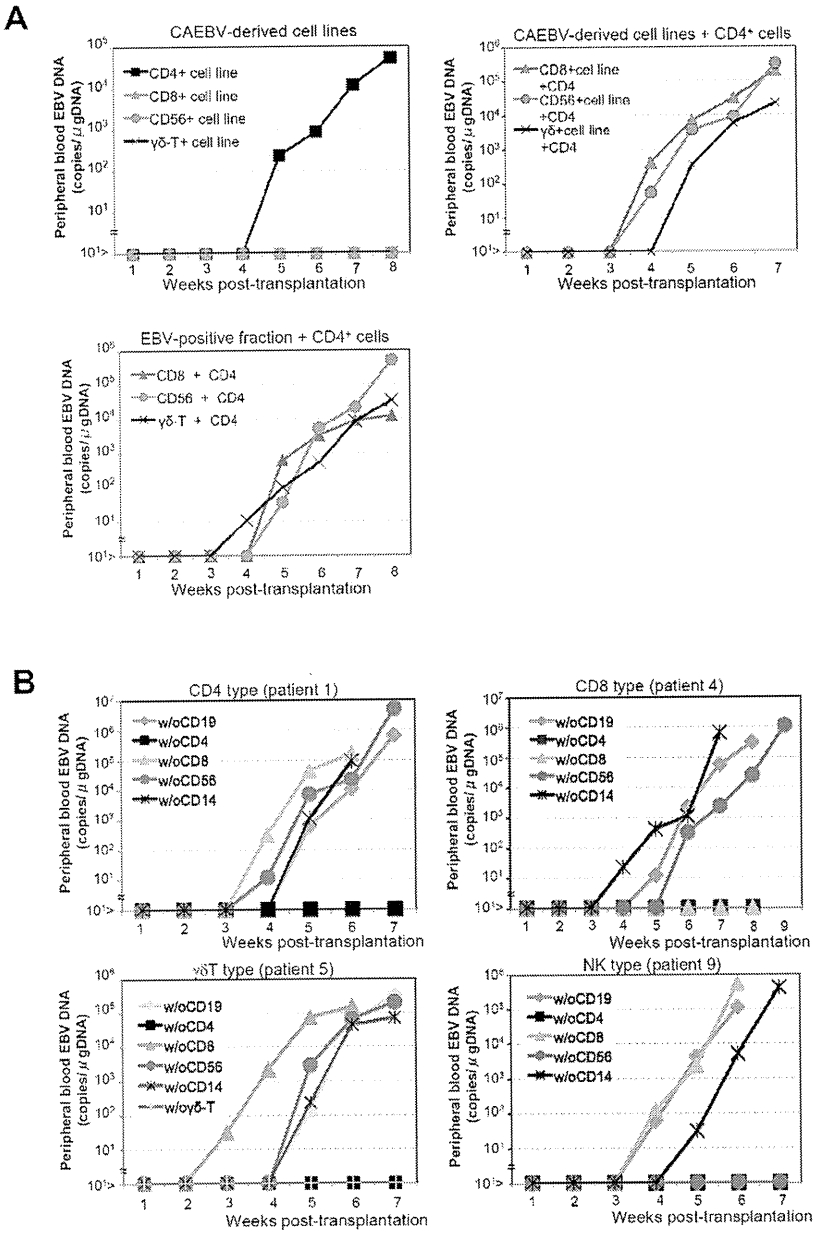


**Figure 3. Analysis on the conditions of the engraftment of EBV-infected T and NK cells in NOG mice.** A. EBV-infected T or NK cells isolated from patients with CAEBV or cell lines derived from them were injected to NOG mice in the conditions described below. Peripheral blood EBV DNA levels were then measured weekly. Upper-left panel: $5\times10^6$ cells of EBV-infected $CD4^+$ T, $CD8^+$ T, γδT, and $CD56^+$ NK cell lines established from the CAEBV patients 1, 4, 6, and 8, respectively, were injected intravenously to NOG mice. Upper-right panel: $5\times10^6$ cells of the $CD8^+$ T, γδT, and $CD56^+$ NK cell lines established from the patients 3, 6, and 8, respectively, were injected intravenously to NOG mice together with autologous $CD4^+$ T cells isolated from $5\times10^6$ PBMC. Bottom panel: $5\times10^6$ cells of the $CD8^+$ T, γδT, and $CD56^+$ NK fractions isolated freshly from the patients 4, 5, and 7, respectively, were injected intravenously to NOG mice together with autologous $CD4^+$ T cells isolated from $5\times10^6$ PBMC. B. Transplantation of PBMC devoid of individual immunophenotypic subsets to NOG mice. $CD19^+$, $CD4^+$, $CD8^+$, $CD56^+$, or $CD14^+$ cells were removed from PBMC obtained from the patient 1 (CD4 type, upper-left panel), 4 (CD8 type, upper-right), 5 (γδT type, bottom-left), and 9 (NK type, bottom-right) and the remaining cells were injected intravenously to NOG mice. Thereafter peripheral blood EBV DNA was determined weekly.
doi:10.1371/journal.ppat.1002326.g003

PBMC from the CAEBV patient 3 (CD8 type). The results are shown in Figure 5A and demonstrate the expression of mRNAs coding for EBNA1, LMP1, LMP2A, and LMP2B, but not for EBNA2. Expression of the EBV-encoded small RNA 1 (EBER1) was also demonstrated. EBNA1 mRNAs transcribed from either the Cp promoter or the Wp promoter were not detected, whereas those transcribed from the Q promoter was abundantly detected. These results indicate that EBV-infected T cells retain the latency